Introduction to Lens Design

José Sasián

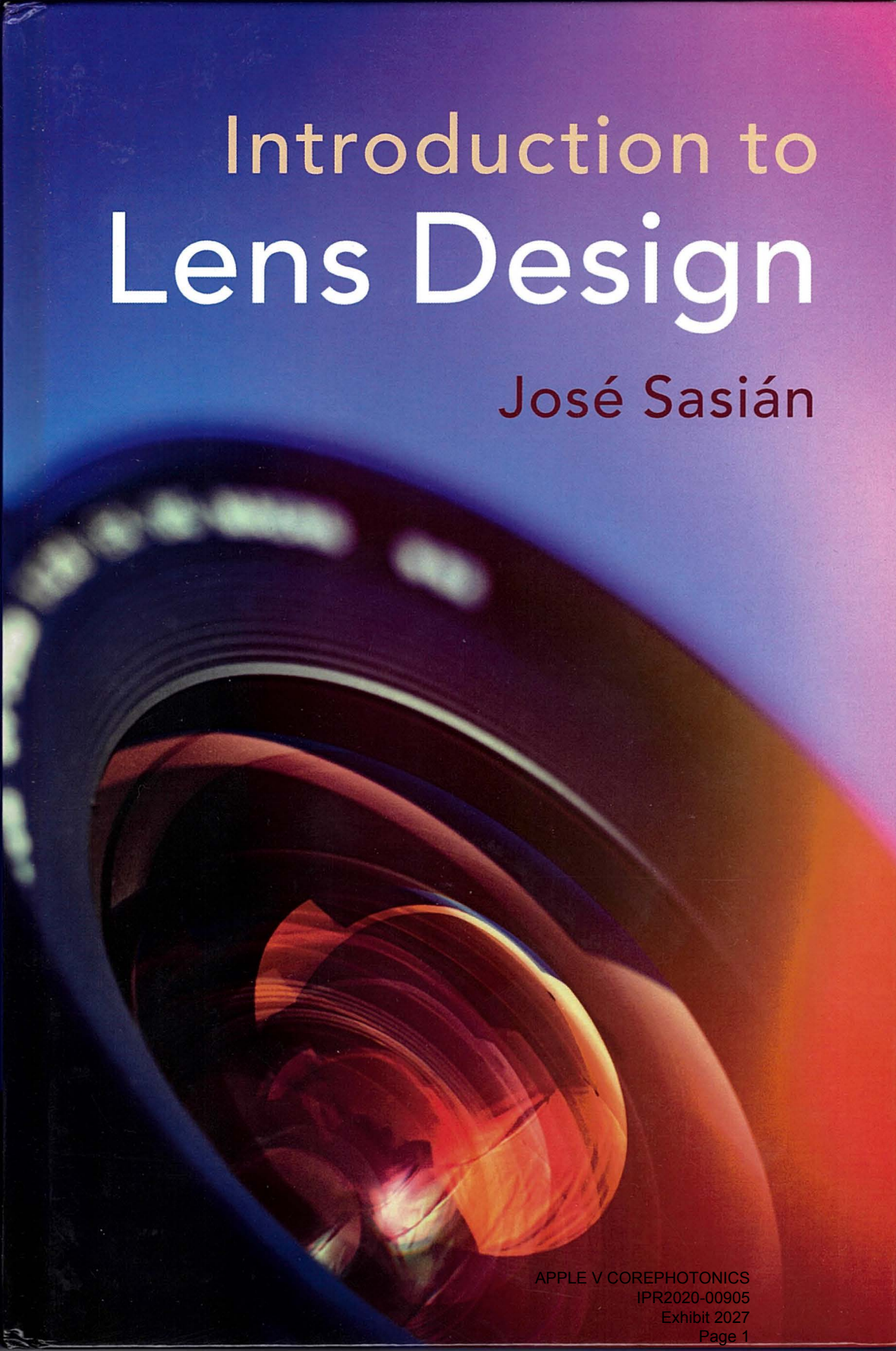

Introduction to Lens Design

Optical lenses have many important applications, from telescopes and spectacles, to microscopes and lasers. This concise, introductory book provides an overview of the subtle art of lens design. It covers the fundamental optical theory, and the practical methods and tools employed in lens design, in a succinct and accessible manner. Topics covered include first-order optics, optical aberrations, achromatic doublets, optical relays, lens tolerances, designing with off-the-shelf lenses, miniature lenses, and zoom lenses. Covering all the key concepts of lens design, and providing suggestions for further reading at the end of each chapter, this book is an essential resource for graduate students working in optics and photonics, as well as for engineers and technicians working in the optics and imaging industries.

JOSÉ SASIÁN is Professor of Optical Design at the James C. Wyant College of Optical Sciences at the University of Arizona in Tucson, AZ. He has taught a course on lens design for more than 20 years and has published extensively in the field. He has worked as a consultant in lens design for the optics industry, and has been responsible for the design of a variety of successful and novel lens systems.

Introduction to Lens Design

JOSÉ SASIÁN
University of Arizona

CAMBRIDGE
UNIVERSITY PRESS

CAMBRIDGE
UNIVERSITY PRESS

University Printing House, Cambridge CB2 8BS, United Kingdom

One Liberty Plaza, 20th Floor, New York, NY 10006, USA

477 Williamstown Road, Port Melbourne, VIC 3207, Australia

314–321, 3rd Floor, Plot 3, Splendor Forum, Jasola District Centre,
New Delhi – 110025, India

79 Anson Road, #06-04/06, Singapore 079906

Cambridge University Press is part of the University of Cambridge.

It furthers the University's mission by disseminating knowledge in the pursuit of education, learning, and research at the highest international levels of excellence.

www.cambridge.org
Information on this title: www.cambridge.org/9781108494328
DOI: 10.1017/9781108625388

First published 2019

Printed in the United Kingdom by TJ International Ltd, Padstow Cornwall

A catalogue record for this publication is available from the British Library.

Library of Congress Cataloging-in-Publication Data
Names: Sasián, José M., author.
Title: Introduction to lens design / José Sasián, University of Arizona.
Description: Cambridge, United Kingdom ; New York, NY, USA : University Printing House, 2019. | Includes bibliographical references and index.
Identifiers: LCCN 2019019484 | ISBN 9781108494328 (hardback)
Subjects: LCSH: Lenses–Design and construction.
Classification: LCC QC385.2.D47 S27 2019 | DDC 681/.423–dc23
LC record available at https://lccn.loc.gov/2019019484

ISBN 978-1-108-49432-8 Hardback

With appreciation to my lens design students.

This is evident even more when we realize that the combinations of lenses are very capricious entities, which in certain arrangements, probably because of laws deeply hidden in the building blocks of complicated functions, will give either not a good image at all, or one that is inevitably curved or distorted, and one understands easily that a lack of knowledge of these laws can lead to high costs and great useless efforts.

Joseph Maximillian Petzval
Bericht über die Ergebnisse einiger dioptrischen Untersuchungen (Pest, 1843)

Contents

Preface

I have been fortunate to have taught for many years the course Lens Design OPTI517 at the James C. Wyant College of Optical Sciences at the University of Arizona. The thrust of this course is to help graduate students to acquire the skill of lens design and obtain a solid foundation in the subject in the space of about 16 weeks, which is the duration of the Fall academic term. Behind the scenes, the challenge has been how to completely and effectively achieve this thrust. This book is the result of teaching OPTI517 for about 20 years, and outlines the essential material interested students or optical engineers should know.

I have had the support and help from many individuals and I would like to acknowledge and to thank them. Robert Shannon handed me OPTI517, which he initiated and taught for many years at the then Optical Sciences Center. My colleagues Russell Chipman, John Greivenkamp, Angus Macleod, Jim Burge, Yuzuru Takashima, Tom Milster, Ron Liang, Buddy Martin, Hong Hua, Jim Schwiegerling, Roland Shack, Masud Mansuripur, Roger Angel, Stanley Pau, Bill Wolfe, Roy Frieden, Brian Anderson, Arvind Marathay, Rolf Binder, Dae Woo Kim, Eustace Dereniak, Steve Jacobs, Harry Barrett, Charles Falco, Jack Gaskill, John Koshel, and Dan Vukobratovich have been helpful and inspirational. I also would like to thank Richard Powell, Jim Wyant, and Tom Koch for the support they have provided me.

I have been fortunate to receive a "yes" when I asked many experts to visit the University of Arizona and help me teach lectures in optical design. Among the many individuals that I can recall and would like to acknowledge and thank are Richard Juergens, Bill Cassarly, Rich Pfisterer, Michael Humphreys, Akash Arora, Vini Mahajan, Richie Youngworth, Richard Buchroeder, Donald Dilworth, Mary Turner, Michael Gauvin, Craig Pansing, Dave Shafer, Jay Wilson, Jake Jacobsen, and John Rogers.

I would like to acknowledge and thank the lens design software companies, Lambda Research Corporation, Optenso™, Optical Systems Design, Inc.,

Synopsis®, and Zemax for always providing excellent academic access to their lens design software and for their outstanding support.

Richard Buchroeder, William Hicks, Craig Pansing, and Jim Schwiegerling provided many useful comments and suggestions to improve several chapters in this book. I am grateful for their help in this endeavor.

I would like thank Nicholas Gibbons, Sarah Lambert, and Roisin Munnelly, at Cambridge University Press, Vinithan Sethumadhavan at SPi-Global, and Liz Steel for their excellent editorial work in publishing this book.

1
Introduction

Lens design is an exciting and important field of optics. This field provides designs for a great diversity of lens and mirror systems needed in many other fields, such as consumer optics, microscope optics, telescope optics, lenses for optical lithography, and photographic optics. Lens and mirror systems are ubiquitous. The work of a lens designer is to provide the constructional data and fabrication tolerances of all the optical elements that a given lens system requires to perform the intended function. Currently many students and engineers are interested in lens design because the field by itself is of great interest, or because they have the need to analyze and design lens systems required in their engineering practice. An optical engineer should have at least some familiarity with how a lens system is designed so that he or she can effectively contribute to develop optical systems.

1.1 Aims of This Book

This book is an introduction to lens design, and has been written to provide an overview of topics that are indispensable to acquire the skill of lens design. Acquiring this skill, the skill of lens design, requires learning some theory, learning how to use lens design software, and gaining experience by designing actual lenses. This book will help the interested reader to understand the theory and methods used in lens design. The book does not have lengthy discussions but, rather, brief discussions to point out essential knowledge. A few references are given for further reading, where the reader can deepen his or her knowledge about a topic.

There are many excellent books about lens design, such as *Lens Design Fundamentals* by Rudolf Kingslake and Barry Johnson, and *Modern Lens Design* by Warren Smith. However, these and other comprehensive books

might not be appropriate for an introduction to lens design, as part of their main focus is the design and survey of a variety of specific lenses. Instead, this introductory book intends to be brief and also to give an overview of topics that a current optical engineer needs to know about lens system design. A graduate student or an optical engineer who understands the content of this book and models, in a lens design program, the different lens systems discussed in it, would then have a solid foundation to practice the skill of lens design. Another aim of this book is to provide an efficient introduction to lens design to an interested student or optical engineer, so that he or she is well positioned to analyze, combine, debug, adjust, or design lens systems.

1.2 Topics Covered

Essential to lens design, and to optical engineering, is an understanding about how optical aberrations are corrected, balanced, or minimized. The reader should have some familiarity with first-order optics and with the theory of optical aberrations, as many discussions revolve about the choices made in the layout of a lens system and how to correct the aberrations. In this book, structural aberration coefficients are used to determine primary aberrations and to understand how to correct, balance, or minimize them. Chapter 2 provides a review of first-order optics and aberrations. Chapter 3 provides a brief discussion of aspheric surfaces. Chapter 4 provides a discussion of thin lenses and how aberrations are controlled in very simple lens systems. Chapter 5 provides a discussion about how ray tracing takes place, and some useful techniques. Chapter 6 provides a discussion about radiometric aspects of a lens system, which are important for a more comprehensive understanding of how lenses work. Chapter 7 discusses achromatic and athermal lenses. Chapter 8 provides a number of lens examples that use combinations of achromatic doublets. This chapter is insightful because it shows how lenses are combined. Chapter 9 discusses the tools used to determine image quality. Chapter 10 discusses how to perform a tolerancing analysis for providing tolerances to the constructional parameters of a lens system that will be manufactured. Chapter 11 comments on issues in using a lens design program. Chapter 12 discusses three classical lenses; the Petzval portrait objective, the Cooke triplet, and the double Gauss lens. Chapter 13 discusses issues that arise in combining lens systems; it also contributes to providing a more comprehensive view about lens systems. Chapter 14 discusses designing with off-the-shelf lenses. Chapter 15 discusses ghost images in a lens system. Chapter 16 discuses some basic mirror systems. Chapter 17 discusses miniature lenses. Chapter 18

provides basic concepts in zoom lens design. In addition to a glossary of terms, the book provides five Appendices, where several tables related to aberrations are provided, as well as a discussion of the sine condition. Thus, the book contents provide a shift in the way lens design is taught. In this introductory book there is more emphasis on providing a broader view of fundamentals and essential topics in lens design, rather than bringing attention to the detailed design of a survey of lenses. This shift responds to current needs in the optical industry, and modern approaches to learning. Yet, this book provides a solid introduction for those who would like to specialize in the art of lens design.

1.3 The Art of Lens Design

There are many types of lens systems, and their variety is increasing with advancements and the creation of new technological fields. Examples of lens types are projection lenses, telephoto lenses, convertible lenses, catadioptric lenses, zoom lenses, underwater lenses, lenses for aerial photography, anamorphic lenses, panoramic lenses, lenses for video and cinematography, lenses for scanning, relay lenses, periscope lenses, and lenses for endoscopes.

The process of lens design starts with understanding the application the intended lens is to be designed for. From understanding the application, the lens specifications list follows. This list of specifications is not always complete or correct. A lens designer must make efforts to verify that the specifications list is as complete and correct as possible. The lens specifications may involve first-order, packaging, image quality, environmental, and lens fabrication constraints and requirements. Once the specifications are understood, the lens designer may start a design from first principles, and by adding complexity to simple lenses. A first-order lens layout can help to visualize a given lens and determine, for example, lens size, element optical power, and type of lens configuration. From the first-order layout, considerations are made about how the aberrations could be corrected. Then a lens design program is used to model and optimize the lens system, and to find alternative lens solutions for comparison. A lens analysis is also made to determine tolerances that a lens manufacturer would need to make the lens elements. A lens design can also start from existing lenses in the patent literature. A lens designer should have effective communication with the opto-mechanical engineer and lens manufacturer to make sure that the designed lens can be mounted in a barrel, fabricated, and assembled. Lens drawings are then drafted. Some optical engineers may not actually design lenses, but would analyze, debug, adjust, and combine existing lens systems. A critical design review is often

held to approve, or disapprove, a lens for fabrication. The overall process of lens design is also of exercising design creativity, and this in part is what makes lens design an exciting field.

Further Reading

Bentley, Julie L., Olson, Craig, Youngworth, Richard N. "In the era of global optimization, the understanding of aberrations remains the key to designing superior optical systems," Proceedings of SPIE 7849, Optical Design and Testing IV, 78490C (2010); doi: 10.1117/12.871720.

Kidger, M. J. "The importance of aberration theory in understanding lens design," *Proceedings of SPIE*, 3190 (1997), 26–33.

Sasián, J. "Trends in teaching lens design," *Proceedings of SPIE*, 4588 (2001), 56–58.

Sasián, José. "From the landscape lens to the planar lens: a reflection on teaching lens design," Proceedings of SPIE 5865, Tribute to Warren Smith: A Legacy in Lens Design and Optical Engineering, 58650I (2005); doi: 10.1117/12.624566.

Shannon, Robert R. "Teaching of lens design," Proceedings of SPIE 1603, Education in Optics (1992); https://doi.org/10.1117/12.57848.

2

Classical Imaging, First-Order Imaging, and Imaging Aberrations

This chapter provides a brief overview of essential imaging concepts used in lens design. Whether classical imaging, which is congruent with first-order optics, is required in a lens system, or any other type of imaging, depends on system application. Therefore, a clear understanding of what imaging is and of departures from such imaging, called aberrations, is essential for a lens design practice.

2.1 Classical Imaging

The main goal in lens design is the design of imaging lenses where images, particularly sharp, are formed. Then it is important to discuss the concept of an image. Depending on application, different imaging concepts can be devised. However, classical imaging, where the image is a scaled copy of the object, is often required for a lens system. The underlying mechanism for classical imaging is central projection. Object points are projected into image points on an image plane, by the line defined by an object point on the object plane and a central projection point pair as shown in Figure 2.1. The projection point pair is the center of perspective and in a lens system, which we assume to have axial symmetry, is represented by a nodal point in object space and its conjugate point, the nodal point in image space. The main attributes of a classical image are its location and its size. The Newtonian or Gaussian imaging equations shown in Table 2.1 permit calculating these attributes and represent central projection imaging.

Ideal imaging as defined by central projection is often a designing goal. For an object at infinity that subtends a semi-field of view, θ, the image height, $\bar{y}_i$, measured from the optical axis, is related to the focal length, f, by the mapping, $\bar{y}_i = f \cdot \tan(\theta)$. However, according to application, there are other

Table 2.1 *Imaging equations*

Newtonian equations	Gaussian equations
$\frac{z}{f} = -\frac{1}{m}$	$\frac{f'}{z'} + \frac{f}{z} = 1$
$\frac{z'}{f'} = -m$	$\frac{z}{f} = 1 - \frac{1}{m}$
$zz' = ff'$	$\frac{z'}{f'} = 1 - m$
The object and image distances z and z' are measured, respectively, from the front and rear focal points. f and f' are the front and rear focal lengths.	The object and image distances z and z' are measured, respectively, from the front and rear principal points. The transverse magnification is m.

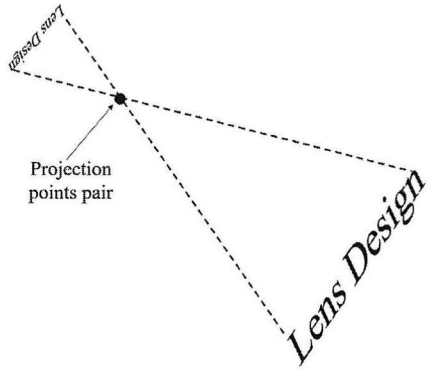

Figure 2.1 Central projection imaging where the object on the left is imaged on the right. In this case the projection points coincide in space.

possible mappings such as the equidistant mapping, $\bar{y}_i = f \cdot \theta$, or the orthographic mapping, $\bar{y}_i = f \cdot \sin(\theta)$. We are assuming that the object and image lay on planes perpendicular to the optical axis of the optical system. There are some applications that require the image to lay on a curved surface, and then the concept of classical imaging no longer applies.

The point is that lenses are designed to produce images which require a lens designer to be clear about what imaging means. Imaging is and will continue to be an important subject which substantially impacts lens design. What imaging is depends on system application.

2.2 First-Order Optics

The concept of first-order imaging arises from a first-order approximation to the path of a real ray. A real ray in homogenous media travels in straight lines,

refracts according to Snell's law, $n' \sin(I') = n \sin(I)$, and its tracing considers the actual shape of the refracting surface. A first-order ray refracts according to a first-order approximation to Snell's law, $n'i' = ni$, and treats the optical surfaces as planar, but with refracting power, ϕ. To trace a first-order ray, the refraction and transfer equations are used:

$$n'u' = nu - y\phi \tag{2.1}$$

$$y' = y + u't, \tag{2.2}$$

where u and u' are the slopes of the ray before and after refraction, y is the ray height at the surface which is assumed planar but with optical power ϕ, n is the index of refraction, and t is the distance to the next surface.

In lens design we are concerned with first-order imaging, as obtained by tracing first-order rays, because it is equivalent to central projection imaging. In addition, first-order imaging establishes a model for a lens system where the cardinal points – these are the focal points, the nodal points, and the principal points – have specific ray properties and serve as useful references. Many calculations in lens design are done by tracing first-order rays and, therefore, an optical designer must be familiar with first-order optics. An example of a calculation in lens design software is what is known as a "solve" in which the program automatically sets the distance t from the last surface to the ideal image plane using $t = -y/u'$.

The space where the object resides is called the object space and is infinite in extent. Similarly, the space where the image resides is called the image space and is infinite in extent. An important structure in a lens system is the aperture stop. The aperture stop is assumed to be circular, to lay on a plane perpendicular to the optical axis, and it solely limits the amount of light for the on-axis beam. The aperture stop helps to well define a lens system; this is, light beams for every field point become well defined after they pass through the aperture stop. The image of the aperture stop in object space is defined as the entrance pupil, and the image of the aperture stop in image space is defined as the exit pupil. The pupils and the stop are optically conjugated, meaning that their locations and sizes satisfy the Newtonian or Gaussian equations that are summarized in Table 2.1. Another aperture that contributes to well define a lens system is the field stop. The field stop limits the field of view of a lens system, and ideally it is located at an image plane.

Rays that travel in a plane that contains the lens system axis of rotational symmetry are called meridional rays. Rays that do not travel in a meridional plane are called skew rays. Two important first-order rays are the marginal and chief rays. By definition, the marginal ray is a meridional ray that originates at the on-axis object point and passes through the edge of the aperture stop. The chief ray is a meridional ray that originates at the edge of the field of view and passes through

Table 2.2 *First-order concepts*

Optical axis	The axis about which an optical system has rotational symmetry.
Object space	The space where the object resides, which is assumed infinite in extent.
Image space	The space where the image resides, which is assumed infinite in extent.
Aperture stop	The aperture that solely limits the amount of light for the axial light beam.
f	Front focal length.
f'	Rear focal length.
Optical power or Refractive power (ϕ)	$\phi = -\frac{n}{f} = \frac{n'}{f'}$; n is the index of refraction in object space, and n' is the index in image space. The unit of power is the diopter or 1/meter.
Effective focal length (EFL)	The inverse of the optical power.
$F/\#$, F-number	The effective focal length divided by the diameter of the entrance pupil. $F/\# = \frac{EFL}{2y_e}$
Lagrange invariant ($\mathcal{H}$)	It relates to the optical throughput or capacity of an optical system to transfer optical power. $\mathcal{H} = n\bar{u}y - nu\bar{y}$
Afocal	The focal lengths are not defined.
Telecentricity in object space	The image of the aperture stop in object space is at infinity. Equivalently, the chief ray in object space is parallel to the optical axis.
Telecentricity in image space	The image of the aperture stop in image space is at infinity. Equivalently, the chief ray in image space is parallel to the optical axis.
Transverse magnification (m)	The first-order ratio of the image size to the object size.

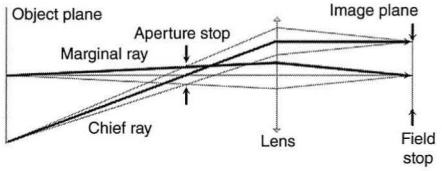

Figure 2.2 The marginal and chief rays (highlighted in bold) in relation to the aperture stop, the object and image planes, the field stop, and an ideal lens.

the center of the aperture stop. The trace of these two rays permits obtaining useful information about the imaging of an optical system. Figure 2.2 shows an object plane, an aperture stop, a lens, an image plane, and two sets of rays defining two light beams for the on-axis object point and for an off-axis point. In particular, Figure 2.2 illustrates the marginal and chief rays using bold rays. Table 2.2 provides a glossary of first-order concepts, and Table 2.3 provides a summary of first-order quantities. The Lagrange invariant, $\mathcal{H}$, is defined by

Table 2.3 *Marginal and chief first-order rays' related quantities*

Item	Marginal ray	Chief ray
Object/pupil distance	s	$\bar{s}$
Image/pupil distance	s'	$\bar{s}'$
Ray slope of incidence	$i = u - \alpha$	$\bar{i} = \bar{u} - \bar{\alpha}$
Ray height at surface	y	$\bar{y}$
	y_e	$\bar{y}_o$
	y_s	$\bar{y}_i$
Ray slope	$u = -y/s$	$\bar{u} = -\bar{y}/\bar{s}$
Normal line slope	$\alpha = -y/r = u - i$	$\bar{\alpha} = -\bar{y}/r = \bar{u} - \bar{i}$
Refraction invariant	$A = ni = n\left(\frac{1}{r} - \frac{1}{s}\right)y$	$\bar{A} = n\bar{i} = n\left(\frac{1}{r} - \frac{1}{\bar{s}}\right)\bar{y}$
Surface radius	r	
Surface vertex curvature	c	
Thickness to next surface	t	
Surface optical power	$\phi = \frac{n'-n}{r}$	
Lagrange invariant	$\mathcal{K} = n\bar{u}y - nu\bar{y} = \bar{A}y - A\bar{y}$	

Quantities related to the chief ray carry a bar.
Primed quantities refer to the image space and un-primed to the object space.

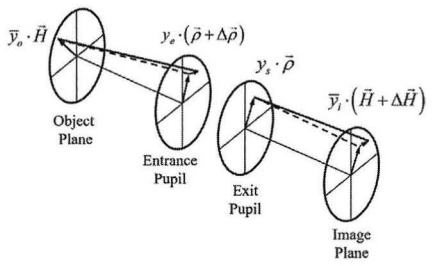

Figure 2.3 Model of an axially symmetric optical system showing the path of a first-order ray and the path of a real ray.

$\mathcal{K} = n\bar{u}y - nu\bar{y}$, using the slope and height of the marginal and chief rays. Its value does not depend on the transverse plane where it is calculated. The amount of optical flux, or optical throughput, $T = \pi^2\mathcal{K}^2$, that can pass through an optical system is proportional to the square of the Lagrange invariant.

Figure 2.3 provides a representation of an optical system where the object and image planes and the entrance and exit pupils are shown. The solid line represents a real ray traveling from the object plane to the image plane, and the broken line represents a first-order ray. Two points are required to define a ray; the first point is defined by the field vector, $\vec{H}$, which lies in the object plane, and the second point is defined by the aperture vector, $\vec{\rho}$, which lies in the exit pupil plane. Both vectors are normalized so their magnitudes range from 0 to 1. To indicate an actual field

point, the field vector is scaled by the chief ray height in object space, $\bar{y}_o$, and the aperture vector is scaled by the marginal ray height, y_s, at the exit pupil. In Figure 2.3 the real ray and the first-order ray coincide necessarily, per definition, at the object plane and at the exit pupil plane. Everywhere else these rays may differ in path. In particular, at the image plane they differ by the vector $\bar{y}_i \Delta \vec{H}$, and at the entrance pupil plane by the vector $y_e \Delta \vec{\rho}$. They differ at the image plane because of image defects known as image aberrations; similarly they differ at the entrance pupil because of pupil aberrations.

A lens designer may start a design with a first-order lens layout, as shown in Figure 2.4. Two ideal lenses with the same focal length form a $4f$ relay, as the distance between object and image is four-times the focal length of the lens elements. Such a layout provides useful information such as the ideal path of rays, the diameter of the lens elements, and the system's size.

In sum, first-order optics is equivalent to classical imaging and provides a basic structure to model a lens system.

2.3 Imaging Aberrations

Actual lens systems do not produce perfect imaging, but introduce image defects known as optical aberrations. Aberration can refer to wave aberration, transverse, longitudinal, or angular ray aberration.

In relation to Figure 2.5 the Optical Path Length (*OPL*) along a ray is defined as,

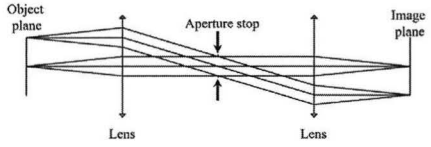

Figure 2.4 A doubly telecentric relay system in a first-order layout. Rays from on-axis and off-axis field points are shown. Two ideal positive lenses are schematically drawn as vertical lines with arrow ends.

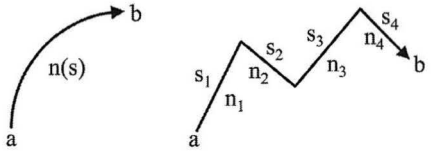

Figure 2.5 Left: Path of a ray in an inhomogeneous medium. Right: Path of a ray in several homogenous media.

$$OPL = \int_a^b n(s)ds, \tag{2.3}$$

where $n(x, y, z)$ is the index of refraction as a function of position, and ds is the element of arc length. If the index of refraction is uniform from medium to medium, then the OPL reduces to a summation over the different media,

$$OPL = \sum_i n_i s_i, \tag{2.4}$$

where n_i is the index of refraction, and s_i is the ray length in medium i. The units of OPL are of length, for example, millimeters. If the OPL is divided by the speed of light, then we obtain a transit time from point a to point b along the ray.

Taking an object point as the origin of rays, the geometrical wavefront is defined as the locus of constant optical path length. As shown in Figure 2.6, in a homogenous medium the wavefront is spherical in shape. However, when the wavefront propagates through an optical system, it is deformed, and its shape is no longer spherical. As the rays are normal to the wavefront, they no longer converge to a sharp image point; i.e., the ideal image point as defined by central projection. In relation to Figure 2.7, the wavefront aberration represents

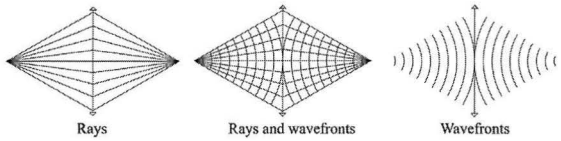

Figure 2.6 Rays and waves which diverge from a point source are refracted by a lens and converge to a point image.

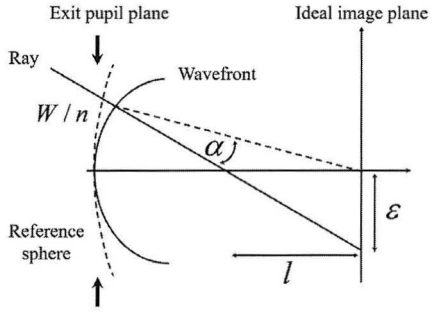

Figure 2.7 Different metrics to refer to aberrations as wavefront deformation, angular ray aberration, transverse ray aberration, or longitudinal ray aberration.

wave deformation, W/n, and the ray error represents angular, α, transverse, ε, or longitudinal, l, aberration.

The wavefront deformation is measured with respect to a reference sphere. As shown in Figure 2.8, the reference sphere is centered at the ideal image point and passes by the on-axis exit pupil point. Note that, because of transverse ray aberration, $\vec{\varepsilon} = \bar{y}_i \Delta \vec{H}$, the ray does not intersect the ideal image point at $\bar{y}_i \vec{H}$. Given a ray defined by the field and aperture vectors $\vec{H}$ and $\vec{\rho}$, the distance along the ray between the reference sphere and the actual wavefront times the index of refraction in image space is the wavefront deformation from the reference sphere for that ray.

For an axially symmetric system the aberration function, $W\left(\vec{H}, \vec{\rho}\right)$, provides the geometrical wavefront deformation at the exit pupil as a function of the normalized field, $\vec{H}$, and aperture, $\vec{\rho}$, vectors. The field vector is located at the object plane and defines where a given ray originates from. The aperture vector defines the intersection of a given ray with the pupil plane. The aperture vector is usually located at the exit pupil plane, but it can also be located at the entrance pupil plane. Figure 2.9 shows in image space the ideal image of the field vector and the aperture vector at the exit pupil plane. The aberration function, being a scalar, involves dot products of the field and aperture vectors, specifically $\vec{H} \cdot \vec{H}$, $\vec{H} \cdot \vec{\rho}$, and $\vec{\rho} \cdot \vec{\rho}$. These dot products only

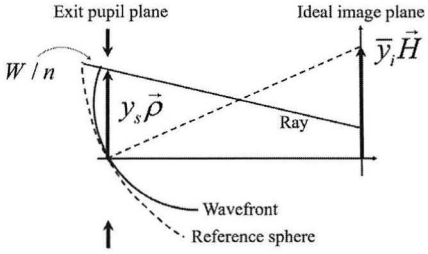

Figure 2.8 The wavefront deformation *W/n* is determined with the aid of a reference sphere.

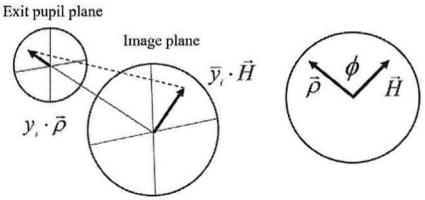

Figure 2.9 The field and aperture vectors (scaled by the marginal ray height at the exit pupil and the chief ray height at the image plane) and the angle between them, looking down the optical axis.

depend on the magnitude of the vectors and on the cosine of the angle, ϕ, between them. The dot products are used to describe axial symmetry, and are known as the rotational invariants, since they do not change their magnitude upon a rotation of the coordinate system about the optical axis.

The aberration function provides the wavefront deformation in terms of optical path, as measured along a particular ray (defined by the tip of the field vector and the tip of the aperture vector) and from the reference sphere to the wavefront. Equivalently, the aberration function provides the Optical Path Difference (*OPD*) between the *OPL* from the object to the wavefront at the exit pupil, and the *OPL* from the object point to the reference sphere. The aberration function is written to sixth-order of approximation as:

$$\begin{aligned} W\left(\vec{H},\vec{\rho}\right) &= \sum_{j,m,n} W_{k,l.m}\left(\vec{H}\cdot\vec{H}\right)^{j}\left(\vec{H}\cdot\vec{\rho}\right)^{m}\left(\vec{\rho}\cdot\vec{\rho}\right)^{n} \\ &= W_{000} + W_{200}\left(\vec{H}\cdot\vec{H}\right) + W_{111}\left(\vec{H}\cdot\vec{\rho}\right) + W_{020}\left(\vec{\rho}\cdot\vec{\rho}\right) \\ &\quad + W_{040}\left(\vec{\rho}\cdot\vec{\rho}\right)^{2} + W_{131}\left(\vec{H}\cdot\vec{\rho}\right)\left(\vec{\rho}\cdot\vec{\rho}\right) + W_{222}\left(\vec{H}\cdot\vec{\rho}\right)^{2} \\ &\quad + W_{220}\left(\vec{H}\cdot\vec{H}\right)\left(\vec{\rho}\cdot\vec{\rho}\right) + W_{311}\left(\vec{H}\cdot\vec{H}\right)\left(\vec{H}\cdot\vec{\rho}\right) + W_{400}\left(\vec{H}\cdot\vec{H}\right)^{2} \\ &\quad + W_{240}\left(\vec{H}\cdot\vec{H}\right)\left(\vec{\rho}\cdot\vec{\rho}\right)^{2} + W_{331}\left(\vec{H}\cdot\vec{H}\right)\left(\vec{H}\cdot\vec{\rho}\right)\left(\vec{\rho}\cdot\vec{\rho}\right) \\ &\quad + W_{422}\left(\vec{H}\cdot\vec{H}\right)\left(\vec{H}\cdot\vec{\rho}\right)^{2} + W_{420}\left(\vec{H}\cdot\vec{H}\right)^{2}\left(\vec{\rho}\cdot\vec{\rho}\right) \\ &\quad + W_{511}\left(\vec{H}\cdot\vec{H}\right)^{2}\left(\vec{H}\cdot\vec{\rho}\right) + W_{600}\left(\vec{H}\cdot\vec{H}\right)^{3} + W_{060}\left(\vec{\rho}\cdot\vec{\rho}\right)^{3} \\ &\quad + W_{151}\left(\vec{H}\cdot\vec{\rho}\right)\left(\vec{\rho}\cdot\vec{\rho}\right)^{2} + W_{242}\left(\vec{H}\cdot\vec{\rho}\right)^{2}\left(\vec{\rho}\cdot\vec{\rho}\right) + W_{333}\left(\vec{H}\cdot\vec{\rho}\right)^{3} \end{aligned} \tag{2.5}$$

where the sub-indices, j, m, n, represent integers, and $k = 2j + m$, $l = 2n + m$, and $W_{k,l,m}$ represent aberration coefficients. The terms in the aberration function represent aberrations, that is, basic forms in which the wavefront can be deformed. The sum of all aberration terms and orders produces the actual total wavefront deformation. The order of an aberration term is given by $2{\cdot}(j + m + n)$, which is always an even order. In the aberration function the field and aperture vectors are normalized so that, when they are unity, the coefficients represent the maximum amplitude of each aberration, which is expressed in wavelengths. The lower indices k, l, m in each coefficient indicate, respectively, the algebraic power of the field vector, the aperture vector, and the cosine of the angle ϕ between these vectors.

Table 2.4 summarizes the first four orders of aberrations using both vector and algebraic expressions. The fourth-order terms are often called the primary aberrations. The ten sixth-order terms can be divided into two groups. The first group (first six terms) can be considered as an improvement upon the primary

Table 2.4 *Wavefront aberrations*

Aberration name	Vector form	Algebraic form	j	m	n
Zero-order					
Uniform piston	W_{000}	W_{000}	0	0	0
Second-order					
Quadratic piston	$W_{200}\left(\vec{H}\cdot\vec{H}\right)$	$W_{200}H^2$	1	0	0
Magnification	$W_{111}\left(\vec{H}\cdot\vec{\rho}\right)$	$W_{111}H\rho\cos(\phi)$	0	1	0
Focus	$W_{020}\left(\vec{\rho}\cdot\vec{\rho}\right)$	$W_{020}\rho^2$	0	0	1
Fourth-order					
Spherical aberration	$W_{040}\left(\vec{\rho}\cdot\vec{\rho}\right)^2$	$W_{040}\rho^4$	0	0	2
Coma	$W_{131}\left(\vec{H}\cdot\vec{\rho}\right)\left(\vec{\rho}\cdot\vec{\rho}\right)$	$W_{131}H\rho^3\cos(\phi)$	0	1	1
Astigmatism	$W_{222}\left(\vec{H}\cdot\vec{\rho}\right)^2$	$W_{222}H^2\rho^2\cos^2(\phi)$	0	2	0
Field curvature	$W_{220}\left(\vec{H}\cdot\vec{H}\right)\left(\vec{\rho}\cdot\vec{\rho}\right)$	$W_{220}H^2\rho^2$	1	0	1
Distortion	$W_{311}\left(\vec{H}\cdot\vec{H}\right)\left(\vec{H}\cdot\vec{\rho}\right)$	$W_{311}H^3\rho\cos(\phi)$	1	1	0
Quartic piston	$W_{400}\left(\vec{H}\cdot\vec{H}\right)^2$	$W_{400}H^4$	2	0	0
Sixth-order					
Oblique spherical aberration	$W_{240}\left(\vec{H}\cdot\vec{H}\right)\left(\vec{\rho}\cdot\vec{\rho}\right)^2$	$W_{240}H^2\rho^4$	1	0	2
Coma	$W_{331}\left(\vec{H}\cdot\vec{H}\right)\left(\vec{H}\cdot\vec{\rho}\right)\left(\vec{\rho}\cdot\vec{\rho}\right)$	$W_{331}H^3\rho^3\cos(\phi)$	1	1	1
Astigmatism	$W_{422}\left(\vec{H}\cdot\vec{H}\right)\left(\vec{H}\cdot\vec{\rho}\right)^2$	$W_{422}H^4\rho^2\cos^2(\phi)$	1	2	0
Field curvature	$W_{420}\left(\vec{H}\cdot\vec{H}\right)^2\left(\vec{\rho}\cdot\vec{\rho}\right)$	$W_{420}H^4\rho^2$	2	0	1
Distortion	$W_{511}\left(\vec{H}\cdot\vec{H}\right)^2\left(\vec{H}\cdot\vec{\rho}\right)$	$W_{511}H^5\rho\cos(\phi)$	2	1	0
Piston	$W_{600}\left(\vec{H}\cdot\vec{H}\right)^3$	$W_{600}H^6$	3	0	0
Spherical aberration	$W_{060}\left(\vec{\rho}\cdot\vec{\rho}\right)^3$	$W_{060}\rho^6$	0	0	3
	$W_{151}\left(\vec{H}\cdot\vec{\rho}\right)\left(\vec{\rho}\cdot\vec{\rho}\right)^2$	$W_{151}H\rho^5\cos(\phi)$	0	1	2
	$W_{242}\left(\vec{H}\cdot\vec{\rho}\right)^2\left(\vec{\rho}\cdot\vec{\rho}\right)$	$W_{242}H^2\rho^4\cos^2(\phi)$	0	2	1
	$W_{333}\left(\vec{H}\cdot\vec{\rho}\right)^3$	$W_{333}H^3\rho^3\cos^3(\phi)$	0	3	0

aberrations by their increased field dependence, and the second group (last four terms) represents new wavefront deformation forms. Figure 2.10 shows the shape (aperture dependence only) of the zero, second, fourth, and the new wavefront shapes of the sixth-order aberrations.

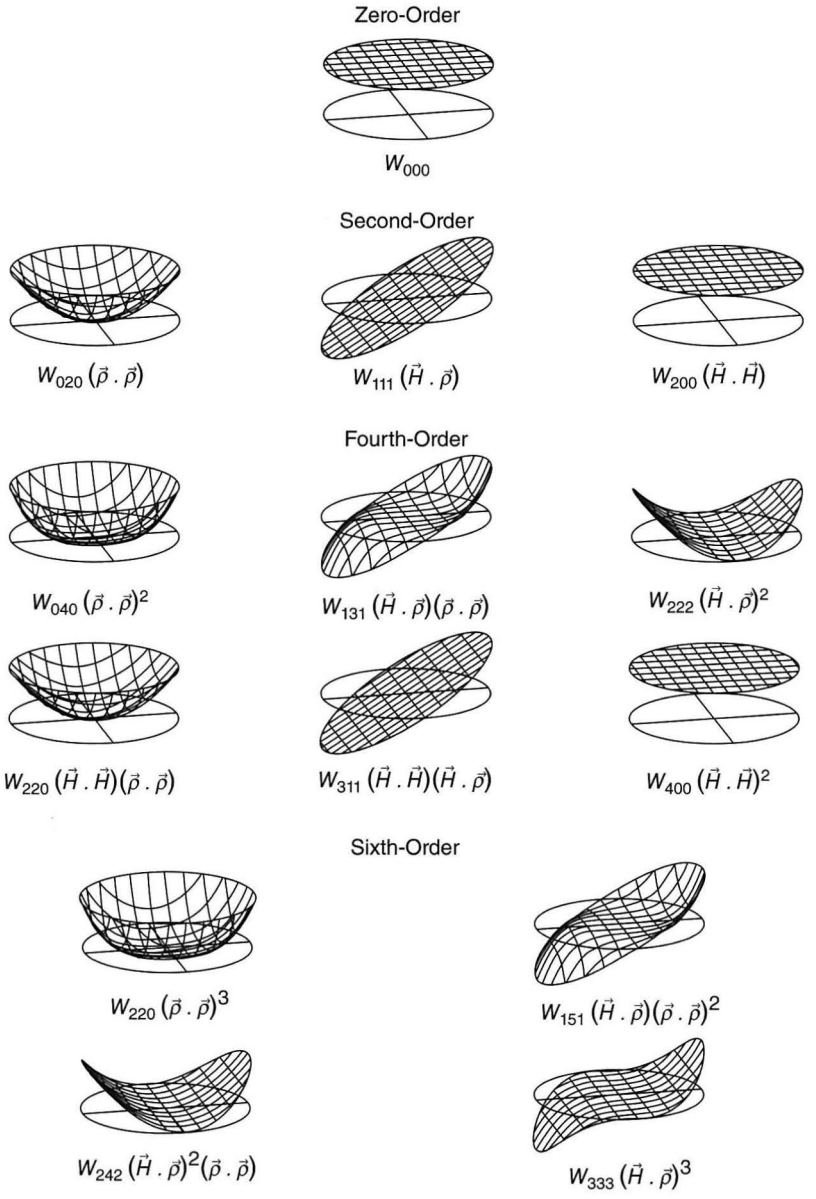

Figure 2.10 Basic wavefront deformation shapes according to symmetry. All of the basic deformations are either axially symmetric, double plane symmetric, or plane symmetric.
(Grid figures with permission and courtesy of Roland Shack.)

Table 2.5 *Aberration coefficients for a system of* j *spherical surfaces in terms of Seidel sums*

Coefficient	Seidel sum
$W_{040} = \frac{1}{8} S_I$	$S_I = -\sum_{i=1}^{j} \left(A^2 y \Delta\left(\frac{u}{n}\right)\right)_i$
$W_{131} = \frac{1}{2} S_{II}$	$S_{II} = -\sum_{i=1}^{j} \left(A \bar{A} y \Delta\left(\frac{u}{n}\right)\right)_i$
$W_{222} = \frac{1}{2} S_{III}$	$S_{III} = -\sum_{i=1}^{j} \left(\bar{A}^2 y \Delta\left(\frac{u}{n}\right)\right)_i$
$W_{220} = \frac{1}{4}(S_{III} + S_{IV})$	$S_{IV} = -\mathcal{H}^2 \sum_{i=1}^{j} P_i$
$W_{311} = \frac{1}{2} S_V$	$S_V = -\sum_{i=1}^{j} \left(\bar{A}\left[\bar{A}^2 \Delta\left(\frac{1}{n^2}\right) y - P(\mathcal{H} + \bar{A}y)\bar{y}\right]\right)_i$

Table 2.6 *Quantities derived from first-order ray data used in computing the aberration coefficients*

Refraction invariant marginal ray	Refraction invariant chief ray	Lagrange invariant	Surface curvature	Petzval sum term
$A = ni = nu + nyc$	$\bar{A} = n\bar{i} = n\bar{u} + n\bar{y}c$	$\mathcal{H} = n\bar{u}y - nu\bar{y}$ $= \bar{A}y - A\bar{y}$	$c = \frac{1}{r}$	$P = c \cdot \Delta\left(\frac{1}{n}\right)$

In Table 2.4, the piston terms represent a uniform phase change across the aperture that does not degrade the image quality. Physically, piston terms represent a time delay or advance in the time of arrival of the wavefront as it propagates from the object to the exit pupil. The second-order term magnification represents a change of magnification, and the focus term represents a change in the axial location of the image. The coefficients for magnification and focus are set to zero given that Gaussian and Newtonian optics accurately predict the size and location of an image. However, a focus term can be added to minimize aberrations or to focus light on a plane other than the ideal image plane.

2.4 Computing Aberration Coefficients

For an optical system made out of j spherical surfaces, the fourth-order aberration coefficients are determined by computing the Seidel sums, S_I, S_{II}, S_{III}, S_{IV}, and S_V. These sums depend only on the Lagrange invariant, and on quantities from a first-order marginal and chief ray trace. Table 2.5 provides

Table 2.7 *Ranges of field of view and relative apertures in lens systems*

Very small	Small	Medium	Large	Very large
FOV				
$< \pm ½°$	$\pm ½°$ to 5°	$\pm 5°$ to 25°	$\pm 25°$ to 45°	$> \pm 45°$
F/#				
< 1	1 to 4	4 to 8	8 to 16	> 16

the Seidel sums formulae, and Table 2.6 provides first-order quantities used in the computation.

In Table 2.5 the operator, $\Delta()$, gives the difference of the argument after and before refraction, this is $\Delta(n) = n' - n$. The summation symbol indicates that the total amount of aberration, for example for spherical aberration W_{040}, is the sum of the spherical aberration contributed by each spherical surface in the system.

2.5 Field of View and Relative Aperture

Two important specifications for a lens system are its field of view (FOV) and its relative aperture (*F/#*). The field of view is the observable scene of a lens system for which it is designed. For a lens that works at finite conjugates, the FOV is specified by the object or image size, and giving the height, width, or both. When the object is at infinity the field of view is usually specified by the semi-angle subtended by the scene, or object, as seen from the entrance pupil, either horizontally, vertically, or both. It can also be specified by the height, width, or both, of the image.

The relative aperture is defined as the ratio of the effective focal length EFL to the diameter of the entrance pupil D_E. Also known as $F/\#$, FNO, *F*-number, and focal ratio *F*. For lens systems that work at finite conjugates the effective relative aperture, sometimes referred to as the working $F/\#$, is given by $F/\# = (1 - m)EFL/D_E$, where m is the transverse magnification.

In a lens that is free from spherical aberration the numerical aperture (NA) is defined by $NA = n \sin(\theta)$, where n is the index of refraction and θ is the angle of the real marginal ray with the optical axis. The *NA* can refer to the object or image spaces. In an aplanatic system the on-axis image brightness is proportional to the square of the numerical aperture, NA^2.

Being aware of the field of view and relative aperture in a lens system is important. Usually, the larger the field of view or the lower the *F/#* is, the more difficult it is to design a lens. Table 2.7 provides ranges of these specifications in lens systems.

Table 2.8 *Doublet lens optical specifications,* $\lambda = 0.6328$ μm

Focal length	*F*-number	Field of view	Aperture stop	Object location	Image quality
100 mm	5	±5°	At doublet	At infinity	Aplanatic

Table 2.9 *Doublet lens prescription*

Surface	Radius	Thickness	Glass
Stop	71.262	4	LAK33
2	−40.363	3	SF6
3	−1,237.921	96.028	Air
Image			Air

Units are millimeters.

Figure 2.11 First-order layout of the doublet lens. Two light beams are shown for the on-axis field point and for the 5 degrees off-axis field point.

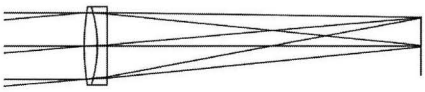

Figure 2.12 Doublet lens drawn with lens surfaces.

2.6 Lens Design Example

A lens designer often starts with the lens specifications. Some important first-order lens specifications are the focal length, the *F*-number, and the field of view. The lens in consideration is a cemented doublet lens corrected for spherical aberration and coma, this is aplanatic. The specifications are given in Table 2.8, and a first-order layout is shown in Figure 2.11.

After a first-order lens layout is created to visualize the lens, a lens designer may substitute ideal lenses for real lenses and correct, balance, or minimize some aberrations. The doublet design is shown in Figure 2.12, where computer optimization was performed to provide a focal length of 100 mm and to correct for spherical aberration W_{040} and coma aberration W_{131}. There are three lens surfaces, and their curvatures are effective variables to satisfy the focal length requirement and the aberration correction.

Table 2.9 provides the doublet lens prescription, Table 2.10 provides a first-order ray trace, and Table 2.11 provides the Seidel sum calculation surface by surface.

Table 2.10 *First-order ray trace*

Surface	y	$n'u'$	$n'i'$	$\bar{y}$	$n'\bar{u}'$	$n'\bar{i}'$
1	10.00	−0.06	0.14	0.00	0.05	0.09
2	9.76	−0.05	−0.53	0.20	0.05	0.08
3	9.60	−0.10	−0.11	0.35	0.09	0.09

Table 2.11 *Doublet lens wave aberration coefficients,* $\lambda = 0.6328$ μm

Surface	W_{040}	W_{131}	W_{222}	W_{220}	W_{311}
1	1.34	3.33	2.08	2.86	3.57
2	−2.90	1.73	−0.26	−0.24	0.07
3	1.56	−5.06	4.10	2.16	−3.49
Total	0.00	0.00	5.92	4.77	0.14

Examination of Table 2.11 shows that surface curvatures were chosen to correct for spherical aberration and coma aberration. There are 5.92 waves of astigmatism aberration and 4.77 waves of field curvature aberration. Distortion aberration is negligible.

2.7 Stop Shifting

Stop shifting is the change of position along the optical axis of the aperture stop to a new location while maintaining the optical throughput, $T = \pi^2 \mathcal{H} K^2$, of the system. This requires maintaining the $F/\#$ and, consequently, the aperture stop must change size. The parameter $\bar{S}$ quantifies stop shifting and can be computed at any surface of the optical system using the old and new quantities at that surface, as indicated by

$$\bar{S} = \frac{\bar{u}_{new} - \bar{u}_{old}}{u} = \frac{\bar{y}_{new} - \bar{y}_{old}}{y} = \frac{\bar{A}_{new} - \bar{A}_{old}}{A}, \tag{2.6}$$

where $\bar{A} = n\bar{i}$ is the refraction invariant for the chief ray, $A = ni$ is the refraction invariant for the marginal ray, $\bar{u}$ is the chief ray slope, u is the marginal ray slope, $\bar{y}$ is the chief ray height at the surface, and y is the marginal ray height at the surface.

A useful set of formulas to determine the change of Seidel sum when the stop aperture is shifted along the optical axis is presented in Table 2.12, where the asterisk indicates the new value for the Seidel sum, and where $\bar{S}$ is the stop shifting parameter.

Table 2.12 *Seidel sums upon stop shifting*

$S_I^* = S_I$
$S_{II}^* = S_{II} + \bar{S}S_I$
$S_{III}^* = S_{III} + 2{\cdot}\bar{S}S_{II} + \bar{S}^2 S_I$
$S_{IV}^* = S_{IV}$
$S_V^* = S_V + \bar{S}(S_{IV} + 3{\cdot}S_{III}) + 3{\cdot}\bar{S}^2 S_{II} + \bar{S}^3 S_I$

Stop shifting formulas provide insight into how aberrations change upon stop shifting whenever there is aberration present in a system. For example, in the presence of spherical aberration, the amount of coma aberration can be changed by stop shifting according to $S_{II}^* = S_{II} + \bar{S}S_I$.

2.8 Parity of the Aberrations and the Principle of Symmetry

The aberrations can be divided into even and odd aberrations depending on the algebraic power of the aperture. The even aberrations are spherical aberration, astigmatism, and field curvature. The odd aberrations are coma and distortion. When there is some lens symmetry about the stop aperture, the odd aberrations tend to cancel, and this provides a mechanism to correct or mitigate the odd aberrations. This is known as the principle of symmetry about the stop.

Further Reading

Greivenkamp, J. *Field Guide to Geometrical Optics* (Bellingham, WA: SPIE Press, 2004).

Sasián, J. *Introduction to Aberrations in Optical Imaging Systems* (Cambridge, UK: Cambridge University Press, 2013).

3

Aspheric Surfaces

Optical systems comprise lenses and mirrors made with precise surfaces. Optical surfaces can be divided into spherical and nonspherical surfaces; the latter are called aspheric surfaces. For a given image quality, the choice of optical surfaces has a major impact on the packaging and cost of a lens system. Therefore, familiarity with types of optical surfaces, with how they can correct aberration, and with their manufacturing and testing methods is important in lens design. This chapter provides an overview of several useful surface types, some of their optical properties, and how they introduce and mitigate aberrations.

3.1 Spherical Surfaces

Spherical surfaces are the preferred optical surfaces because they are relatively easy to manufacture and are described by the equation, $r^2 = x^2 + y^2 + (z - r)^2$, where r is the radius of curvature. The reason for their ease of manufacturing is that two spherical surfaces of the same radius, one concave and one convex, fit each other regardless of their relative position. In traditional optics fabrication, two surfaces are rubbed against each other in the presence of an abrasive, and naturally they tend to conform to each other, acquiring a spherical form. Because of the ease of fabrication and testing, spherical surfaces are the default surfaces in lens design. Optically a spherical surface is specified by its radius of curvature, r, and its clear aperture.

Surfaces that are not spherical are called aspherical, and we assume that they have an axis of rotational symmetry. Specifically, their $sag(x^2 + y^2)$, or depth, z, depends on the radial distance, $\sqrt{x^2 + y^2}$, to the axis of rotation or the optical axis, which coincides with the z coordinate axis.

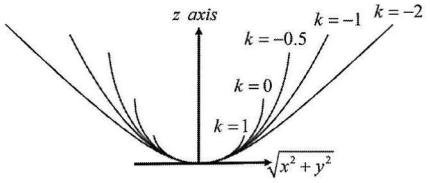

Figure 3.1 Cross-sections of conicoids with the same vertex radius of curvature and according to the conic constant k.

3.2 Conicoids

By rotating the conic sections about their axes, surfaces of revolution called conicoids, or conoids, are generated. These are described by their vertex radius of curvature, r, and their conic constant, $k = -\varepsilon^2$, where ε is the eccentricity. Unlike the sphere, the ellipsoid, the paraboloid, and the hyperboloid surfaces possess two separated optical foci. Light from a point source located at one focus, after reflection on the conicoid, converges to or appears to diverge from the other focal point.

In optical design, the sag of a conic surface is expressed by,

$$sag(x^2+y^2) = z(x^2+y^2) = \frac{c(x^2+y^2)}{1+\sqrt{1-(1+k)(x^2+y^2)c^2}}, \tag{3.1}$$

where $c = 1/r$ is the vertex curvature of the surface. As shown in Figure 3.1, depending on the value of the conic constant k, the surface can be a sphere, $k = 0$; a paraboloid, $k = -1$; an ellipsoid, $-1 < k < 0$; a hyperboloid, $k < -1$; or a spheroid, $k > 0$. The equation of a conic is of second order, and it is possible to find the intersection point of a ray in closed mathematical form.

Within the fourth-order theory of aberrations, the correction of spherical aberration by a surface requires,

$$W_{040} = -\frac{1}{8}A^2 y \Delta\left(\frac{u}{n}\right) - \frac{1}{8}kc^3 y^4 \Delta(n) = 0. \tag{3.2}$$

Then for an object at infinity we must have,

$$k = -\left(\frac{n}{n'}\right)^2. \tag{3.3}$$

As shown in Figure 3.2, when $n' = 1$ there is no spherical aberration if $k = -n^2$, which requires a hyperboloid surface. When $n = 1$ there is no spherical aberration if $k = -1/n'^2$, which requires an ellipsoidal surface.

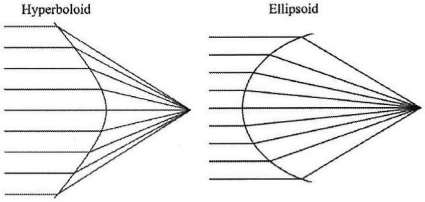

Figure 3.2 Left: Light refraction by a hyperboloid surface with $n = 1.5$, $n' = 1$, and $k = -2.25$. Right: Light refraction by an ellipsoid surface with $n = 1$, $n' = 1.5$, and $k = -0.4444$.

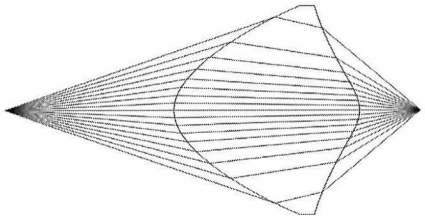

Figure 3.3 A lens with Cartesian surfaces forming a point image from a point object source.

For light reflection on a mirror surface to have no spherical aberration we must require,

$$k = -\left(\frac{1+m}{1-m}\right)^2, \tag{3.4}$$

where m is the transverse magnification.

3.3 Cartesian Ovals

Cartesian ovals are curves or surfaces defined by using two points, one in object space, $s(0,0,s)$, the other in image space, $s'(0,0,s')$, and by requiring that the optical path length for any ray from the object to a surface point, $p(x_p, y_p, z_p)$, and to the image point be constant. Mathematically, Cartesian ovals are defined by,

$$n's' - ns = n'\sqrt{x_p^2 + y_p^2 + (z_p - s')^2} + n\sqrt{x_p^2 + y_p^2 + (z_p - s)^2}, \tag{3.5}$$

where n and n' are the indices of refraction in object and image spaces, respectively. Cartesian ovals produce, geometrically, a perfect on-axis point image free from spherical aberration. Figure 3.3 shows a lens with Cartesian

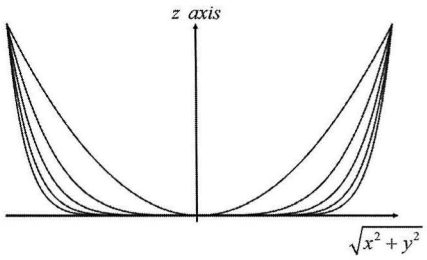

Figure 3.4 Monomials x^2+y^2, $(x^2+y^2)^2$, $(x^2+y^2)^3$, $(x^2+y^2)^4$, and $(x^2+y^2)^5$.

ovals as surfaces. In some cases Cartesian ovals become conicoids, such as in reflection or when one of the defining points is at infinity.

3.4 Polynomial Surfaces

To extend the modeling capabilities, polynomial surfaces are also used in lens design. The sag of a polynomial surface is given by,

$$sag(x^2+y^2) = A_2(x^2+y^2) + A_4(x^2+y^2)^2 + A_6(x^2+y^2)^3 + \cdots, \quad (3.6)$$

where A_2, A_4, and A_6 are the second, fourth, and sixth-order coefficients of asphericity, respectively. Figure 3.4 shows the cross-sections of the monomials, x^2+y^2, $(x^2+y^2)^2$, $(x^2+y^2)^3$, $(x^2+y^2)^4$, and $(x^2+y^2)^5$. Note that, as the algebraic order increases, most of the asphericity takes place toward the surface edge.

For many practical lens design problems, the superposition of a conicoid and a polynomial surface provides substantial flexibility to model optical surfaces, this is,

$$sag(x^2+y^2) = \frac{c(x^2+y^2)}{1+\sqrt{1-(1+k)(x^2+y^2)c^2}} + A_2(x^2+y^2) + A_4(x^2+y^2)^2 + A_6(x^2+y^2)^3 + \cdots. \quad (3.7)$$

Usually the second-order coefficient of asphericity, A_2, is not used simultaneously with the vertex radius of curvature, $r = 1/c$, as first-order properties would depend on both r and A_2. The number of aspheric coefficients used depends on the polynomial convergence to find the ideal surface needed, and on the ability of the lens design optimizer to find a solution. In a polynomial surface the algebraic order of the monomials can be even, or even and odd.

Table 3.1 *Contributions to the Seidel sums from an aspheric surface with conic constant, k, and fourth-order coefficient of asphericity, A_4*

$\delta S_I = a$	$\delta S_{II} = \left(\frac{\bar{y}}{y}\right) a$	$\delta S_{III} = \left(\frac{\bar{y}}{y}\right)^2 a$
$\delta S_{IV} = 0$	$\delta S_V = \left(\frac{\bar{y}}{y}\right)^3 a$	$a = \left(-kc^3 + 8A_4\right) y^4 \Delta(n)$

Adding odd monomials to a surface description enhances its modeling capabilities; for example, a conical surface can be modeled with the term, $\sqrt{x^2 + y^2}$. The sag of an odd and even polynomial aspheric surface is,

$$sag\left(x^2 + y^2\right) = \frac{c(x^2 + y^2)}{1 + \sqrt{1 - (1 + k)(x^2 + y^2)c^2}} + A_1\sqrt{x^2 + y^2} + A_2\sqrt{x^2 + y^2}^2 + A_3\sqrt{x^2 + y^2}^3 + A_4\sqrt{x^2 + y^2}^4 + A_5\sqrt{x^2 + y^2}^5 + A_6\sqrt{x^2 + y^2}^6 + \cdots. \tag{3.8}$$

In the presence of a polynomial surface there is no closed form solution to the intersection point of a ray, and therefore an iterative procedure is used to find the intersection point to a high degree of accuracy. Aspheric surfaces can often lead to better optical performance, to size and weight reduction of an optical system, and, in some cases, to unique solutions to certain design problems. Depending on the application, aspheric surfaces can be cost effective, such as in plastic optical systems that are mass produced. For ease of fabrication and testing, spherical surfaces are the default surfaces to be specified, then conicoids, Cartesian ovals, and last polynomial surfaces. An aspheric surface is specified by its nominal vertex radius of curvature, conic constant, aspheric coefficients, and diameter.

3.5 Aberration Coefficients

The contributions to the Seidel sums from an aspheric surface specified with the vertex radius of curvature, $r = 1/c$, conic constant, k, and fourth-order coefficient of asphericity, A_4, are given in Table 3.1. An aspheric surface is thought of as the superposition of a sphere of radius r, and an aspheric cap defined by k and A_4. The fourth-order aberration contributed by the aspheric surface is the sum of the aberration by the spherical part, for example, S_I, for spherical aberration, and for the aspheric cap, δS_I.

The ratio of the chief ray height to the marginal ray height, $\bar{y}/y$, at the aspheric surface determines whether the surface will contribute only spherical

aberration ($\bar{y}/y = 0$), or in addition coma, astigmatism, and distortion ($\bar{y}/y \neq 0$). When an aspheric surface is located at the aperture stop, or at a pupil, spherical aberration W_{040} is the only contribution of fourth-order.

3.6 Testing Aspheric Surfaces

Whenever an aspheric surface is specified it is necessary to determine how that surface could be tested. As an example, a paraboloid mirror has applications in astronomical telescopes, and a null corrector is often used for its testing. Light from a point source illuminates and passes through a lens system, called a null corrector, then it reaches the aspheric surface under test where the light is reflected, then passes a second time through the null corrector, and finally forms a point image. Any error on the surface of the mirror, called a figure error, produces an aberration in the point image and provides information about how to polish the mirror to correct its optical figure error. Since light passes twice through the null corrector, the configuration is referred to as a *double pass*.

An easy way to design a null corrector is in a *single pass*. As shown in Figure 3.5, light rays from a point at infinity are refracted by a paraboloid surface and become coincident with the normal lines to the paraboloid. This is modeled in a lens design program by setting the index of refraction prior to the paraboloid equal to $n = 1 \times 10^{-8}$. Since the index of refraction in object space is nearly zero, then the angle of refraction is nearly zero, and the refracted rays must coincide with the normal lines to the paraboloid. The refracted rays suffer from negative spherical aberration and form a ray caustic at the mirror vertex's center of curvature where a field lens is located. Then a relay lens is placed to form a point image. The negative spherical aberration from the paraboloid surface is compensated with the positive spherical aberration from the relay lens, which has spherical surfaces for ease of fabrication, characterization, and testing.

Near the ray caustic the ray height is non-linear, and for low *F/#* mirrors a single relay lens would not adequately compensate for aberrations, as also

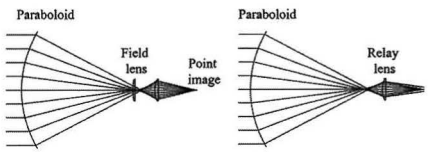

Figure 3.5 Testing a paraboloid mirror. Left: Schematic of an Offner null corrector. Right: Single relay lens null corrector.

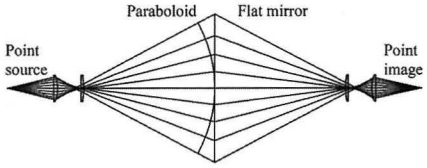

Figure 3.6 Schematic of an Offner null corrector in double pass. In modeling the test configuration with lens design software, a flat mirror has been added to unfold the path of light. This unfolding is not physically possible, but can be done in ray tracing.

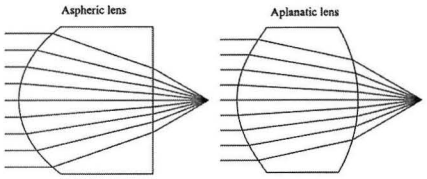

Figure 3.7 Left: An aspheric plano-convex lens corrected for spherical aberration. Right: A double convex aspheric lens corrected for spherical and coma aberration.

shown in Figure 3.5. The field lens redistributes the rays at the relay lens so that their height becomes more linear, allowing for a good match between the aberration from the paraboloid and the aberration from the relay lens. The field lens creates an image of the surface under test on the relay lens and controls higher order spherical aberration. Once a null corrector is designed in a single pass, it can be verified in a double pass, as shown in Figure 3.6.

3.7 Control of Spherical Aberration

Aspheric surfaces provide effective degrees of freedom to correct all orders of spherical aberration. Figure 3.7 shows a light focusing plano-convex lens free from spherical aberration. The convex surface uses an elliptical surface defined with a conic constant, k, and a fourth-order coefficient of asphericity, A_4. In this case only two coefficients are needed to provide satisfactory correction. However, if no conic constant is used, then up to fourteenth order aspheric coefficients are needed to properly correct for spherical aberration. This is due to the lack of fast convergence of the polynomial surface for this single lens design. For ease of alignment the lens must be corrected also for coma aberration so that a small field of view with excellent image quality is provided. This can be done by using the index of refraction as a second degree of freedom, or

by using the curvature of the second surface, as also shown in Figure 3.7. When a lens system is corrected for both spherical aberration and coma aberration, it is referred to as an aplanatic lens.

Since spherical aberration depends on the fourth-order of the lens aperture, it is often best to correct for it at a location in a lens system where the marginal ray height is maximum. In addition, in order to not introduce other fourth-order aberrations, spherical aberration is often corrected by an aspheric surface that coincides, or is near, the aperture stop or a pupil.

3.8 Freeform Surfaces

The lens systems that are discussed in this book are mainly axially symmetric. However, if the axial symmetry in a lens system is not retained, new design possibilities and solutions to imaging problems result. Such non-axially symmetric lens systems also benefit from aspheric surfaces and, because these surfaces have at most one plane of symmetry and provide enhanced degrees of freedom to correct aberration, they are called freeform surfaces.

A freeform surface does not have axial or translational symmetry. Two cylindrical surfaces of the same radius fit to each other if they are translated along the cylinder axis, or translated perpendicular to the axis. Thus, cylindrical surfaces have translational symmetry, and have two orthogonal planes of symmetry. An axially symmetric surface has an infinite number of planes of symmetry, i.e., any meridional plane. Thus, a freeform surface is aspheric and has no more than one plane of symmetry.

Freeform surfaces are used in lens and mirror systems that do not have axial symmetry. These systems can have, in addition to spherical aberration, uniform astigmatism and uniform coma aberration over the field of view. The aberrations that plane symmetric systems can have are given in Appendix 4.

A useful freeform surface is defined by the superposition of a conic surface and a plane symmetric polynomial, symmetric about the Z–Y plane. The sag is,

$$sag(x^2, y) = \frac{c(x^2 + y^2)}{1 + \sqrt{1 - (1 + k)(x^2 + y^2)c^2}} + A_2(x^2) + A_3(x^2 + y^2)y + A_4(x^2 + y^2)^2 + \cdots. \tag{3.9}$$

The term, $A_2(x^2)$, adds a cylindrical deformation which is useful in controlling uniform astigmatism. The term, $A_3(x^2 + y^2)y$. is a cubic deformation which is useful for controlling uniform coma aberration. The term, $A_4(x^2 + y^2)^2$, is axially symmetric, and is useful for controlling spherical aberration.

3.9 User Defined Surfaces

For certain design problems, standard aspheric surfaces do not provide a solution because of a slow convergence and a limited number of aspheric terms. Then it is possible to write the code for a user defined surface to be used by lens design software. Writing the computer code for such a surface requires coming up with a potential surface type, producing the mathematical equations that describe that surface, finding the normal line at each surface point, performing refraction or reflection, and then compiling the code.

Further Reading

Brauneckeer, B., Hentschel, R., Tiziani, H. J. *Advanced Optics Using Aspherical Elements* (Bellingham, WA: SPIE Press, 2008).

Forbes, G. W. "Shape specification for axially symmetric optical surfaces," *Optics Express*, 15 (2007), 5218–26.

Greynolds, Alan W. "Superconic and subconic surface descriptions in optical design," Proceedings of SPIE 4832, International Optical Design Conference 2002 (December 23, 2002).

Hsueh, Chun-Che, Elazhary, Tamer, Nakano, Masatsugu, Sasián, José. "Closed-form sag solutions for Cartesian oval surfaces," *Journal of Optics*, 40(4) (2011), 168–75.

Offner, Abe. "A null corrector for testing paraboloidal mirrors," *Applied Optics*, 2(2) (1963), 153–55.

Reshidko, Dmitry, Sasián, José. "A method for the design of unsymmetrical optical systems using freeform surfaces," Proceedings of SPIE 10590, International Optical Design Conference 2017, 10590V (2017).

Sasián, José. "Design of null correctors for the testing of astronomical optics," *Optical Engineering*, 27(12) (1988), 121051.

Sasián, José, Reshidko, Dmitry, Li, Chia-Ling. "Aspheric/freeform optical surface description for controlling illumination from point-like light sources," *Optical Engineering*, 55(11) (2016), 115104.

Shultz, G. *Aspheric Surfaces*, Progress in Optics, Vol. XXV (Amsterdam: Elsevier, 1988), 349–415.

10

Lens Tolerancing

A lens manufacturer requires tolerances in the dimensions of a lens to be able to provide a cost estimate and be able to manufacture the lens. Further, for the lens to meet the lens specifications after it is built, it is necessary that the actual lens dimensions do not depart from the nominal design ones by some amounts known as fabrication and assembly tolerances. Thus, the task of the lens designer is not only to provide a lens design that meets image quality requirements, but to also provide tolerances, so that the as-built lens actually meets the specifications and satisfies the needs of the application. Critical goals of the lens tolerancing process are to provide tolerances to each of the constructional parameters of the lens, and to find out the statistics of the as-built lens so that the fabrication yield, and final cost, can be estimated. This chapter provides a primer into the lens tolerancing process. Commercial lens design software allows for the lens tolerancing analyses discussed below.

10.1 Lens Dimensions and Tolerances

A lens designer needs to develop an understanding of physical dimensions and their measurement so that realistic tolerances can be assigned. He or she needs to have insight into linear and angular dimensions, such as how big a micrometer is, or one-arc second is. In lens fabrication, both of these magnitudes often separate what is very difficult to make from what is reasonable to make. One must find out how a given lens dimension will be achieved and measured in the optics shop. If it cannot be measured, it probably cannot be made to specification.

Twenty-five micrometers (25 μm) is a useful reference. The minimum measurement division of many instruments and machining tools is $0.001''$, or about 25 μm. Asking for an optical element to be made with a tolerance of

Table 10.1 *Tolerance guidelines for glass lenses, 10 mm to 100 mm in diameter*

Lens parameter	Low precision	Precise	High precision	Requires special process
Diameter (mm)	+0.0 −0.25	+0.0 −0.1	+0.0 −0.025	+0.0 −0.005
Central thickness (mm)	±0.12	±0.05	±0.012	±0.002
Edge thickness difference (mm)	0.12	0.012	0.006	0.003
Surface radius (rings)	5% (10)	1% (3–5)	0.1% (1)	0.01% (0.25)
Wavefront error from surface figure	0.5λ RMS	0.07λ RMS	0.04λ RMS	0.02λ RMS

25 μm is considered doable. Asking for that element to be made to 50 μm or more is considered easy. However, asking for an optical part to be made to 12.5 μm starts to become difficult, to 2.5 μm becomes very difficult, and to 0.25 μm extremely difficult. Similarly, by dividing 25 μm over a lens diameter of 25 mm, we get an angular tolerance of about 3.3 arc-minutes, which is doable. One order of magnitude up or down makes the angular tolerance easy or difficult to achieve.

Different optics shops can make a given lens dimension, such as lens diameter, lens thickness, surface radius, or wedge between the lens surfaces, with a tight tolerance for a given cost, or cannot achieve a given tolerance. The lens designer needs to have effective communication with the lens manufacturers, to find out how well they can achieve lens tolerances, and their associated cost. Lens manufacturers provide guidelines for the different lens tolerances they can achieve under some assumptions. Generally, the tighter the tolerances, the costlier the lens becomes. What a tight tolerance is also depends on the manufacturing process. For example, state-of-the-art, mass produced injection molded lenses for mobile phones routinely achieve micrometer level tolerances. Table 10.1 provides some guidelines for the level of tolerances for lenses with spherical surfaces in the order of 10–100 mm in diameter, made out of glass, and which are not mass produced.

The lens diameter refers to the actual lens diameter, in comparison to the clear aperture of the lens that performs the optical function of refracting or reflecting light rays. A common surface polishing problem is to have the very edge of the surface turned down. To overcome this figuring problem, there is a tendency to specify a lens diameter larger, say 10–20% larger, than the clear aperture. However, usually packaging requirements and lens cost win and the

diameter of the lens is minimized to only allow for enough clearance to properly mount the lens. It is imperative that a bevel, or protective chamfer, is specified to avoid the lens edge easily chipping.

The central lens thickness is measured from surface center to surface center, i.e. along the optical axis. Measuring central thickness requires finding the central portion of the lens, and this contributes to making a precise measurement difficult.

Edge thickness difference, or lens wedge, is measured by supporting the lens in a kinematical mount so that its position is well-defined, and rotating the lens while a micrometer measures the position of the lens edge as the lens rotates. This produces the micrometer reading to oscillate between a minimum and a maximum value, which is the edge thickness difference, called the total indicator runoff. This difference, divided by the lens diameter, gives the lens wedge.

Measuring the radius of curvature of a surface requires an optical bench. Alternatively, optics shops have a collection of test plates with radii of curvature measured with accuracy in an optical bench. Then the lens designer, in a final lens optimization run, fits the radii of curvature of the surfaces of the lens to the radii of curvature of the optics shop test plates. The optics shop tests for radii of curvature errors by observing the Newton rings formed by the test plate and a given lens surface. In this method, the surface radius of curvature is given a tolerance in Newton rings at a given wavelength of light. One Newton ring represents $1/2\lambda$ of sag difference at the edge of the lens between the test plate and the lens surface.

Surface figure, or irregularity, refers to the departure of a surface from the spherical shape, or from the nominal designed aspheric shape. There are many types of figure error, such as surface cylindrical deformation, which would introduce astigmatism aberration, an axially symmetrical error, which would introduce spherical aberration, such as turned down edge, periodic surface errors, which could diffract light and introduce image artifacts, asymmetric surface errors, and others. These figure errors depend on the lens manufacturing method. For example, single point diamond turning produces periodic high spatial frequency figure errors.

A change in the glass index of refraction of a lens element will change the first-order properties of a lens system and will introduce wavefront changes. A change in the glass ν-number of a lens element will change the chromatic correction. To minimize errors, the index of refraction of the glass to be used in the lens manufacture is measured, and the lens is re-optimized to reflect the actual index of refraction. For optical systems with glass elements larger than about 80 mm in diameter, and that are diffraction limited, index of refraction homogeneity within the glass is also a concern.

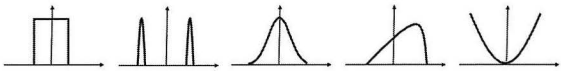

Figure 10.1 Parameter error distributions. From left to right, uniform, end limited, truncated normal, skewed, parabolic.

Each of the constructional parameters of a lens can have a given error distribution. For example, the error in central lens thickness may be biased to the thicker side to allow room for regrinding a lens in case the surface becomes scratched. Some parameter error distributions are uniform, end-limited, truncated normal, shifted-skewed, and parabolic, as shown in Figure 10.1.

10.2 Worst Case

It is perhaps tempting to try to determine the worst case performance of a lens that will be manufactured under a variety of fabrication errors. Determining the worst case estimate is not practical, because it would require us to compute the effects of all combinations of errors, and this can take an excessive amount of time, even for simple systems.

Alternatively, if there are, say, n causes of errors, a worst case can be set by adding all the effects of the errors in the same direction. However, this approach is pessimistic.

Therefore, the approach that is taken in practice for tolerancing is statistical in nature. Consequently, one goal in tolerancing a lens is to estimate the statistics of the as-built lens.

10.3 Sensitivity Analysis

For tolerancing a lens it is necessary to define a criterion of performance such as, for example, the error function used to optimize the lens. It is important to properly reflect relevant aspects of the lens in the tolerancing criterion. An insufficient criterion may lead to a faulty tolerancing analysis.

A sensitivity analysis uses a list of all the constructional parameters that can have actual fabrication errors, such as lens thickness, lens spacing, surface curvature, and index of refraction. Then, tolerances are assigned and used to vary the constructional parameters of a lens, one at each time, and determine how much the tolerancing criterion has changed. This is done for each of the

Table 10.2 *Sensitivity analysis*

Surface	Item	Nominal value	Tolerance	Criterion change
1	Radius	50 mm	0.01 mm	0.3
2	Thickness	8 mm	0.1 mm	0.005
3	Index	1.51	0.001	0.001

Table 10.3 *Inverse sensitivity analysis*

Surface	Item	Nominal value	Tolerance	Criterion change
1	Radius	50 mm	0.003 mm	0.01
2	Thickness	8 mm	0.2 mm	0.01
3	Index	1.51	0.01	0.01

constructional parameters, and the changes in the criterion are ranked to determine which parameters produce the larger changes in the criterion. Table 10.2 provides an example of the data produced in a sensitivity analysis.

A sensitivity analysis produces two useful pieces of information: the lens parameters that worst offend the performance of the lens, and the criterion changes which can be used to estimate the statistics of the as-built lens.

10.4 Inverse Sensitivity Analysis

In an inverse sensitivity analysis, tolerances are determined that would produce a given change in the tolerancing criterion. Table 10.3 provide an example of the data produced in an inverse sensitivity analysis. Such analyses provide information about the levels of tolerance needed for a given performance, and indicate which parameters require loose or tight tolerances.

10.5 Compensators

In order to relax tolerances and reduce manufacturing cost, some compensators such as an air-space, or a lens decenter, can be used to improve a lens system after the lens elements have been made. For example, the back focal length is used to best focus the image, and an airspace can be used to restore the focal length or to correct for residual spherical aberration. However, for mass produced lenses, it is desirable to not specify compensators, as their

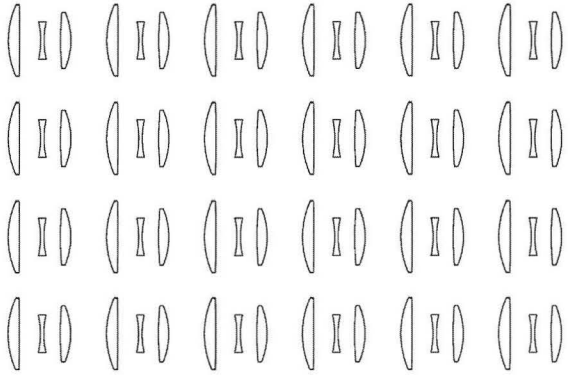

Figure 10.2 Twenty-four Cooke triplet lenses

implementation requires testing and time to fix the problem. Best focusing of the lens by moving the lens assembly, or the image sensor, is most often specified as a compensator.

10.6 Tolerancing Criterion Statistics

Often lenses are manufactured in bulk, and the quality of each lens differs among the lenses because the manufacturing errors are not the same for all the lenses. Or, even, a single lens system where the lens is disassembled and reassembled, can result in a different lens because the lens element positions and air spaces vary. Figure 10.2 shows twenty-four Cooke triplet lenses. If the performance of these lenses were to be measured, one would find variation in the focal length and in the image quality.

Theory shows that, when the manufacturing errors are very small, and for a given tolerancing criterion such as the RMS spot size, or RMS wavefront error, the histogram for a large number of lenses approaches a normal probability distribution, as shown in Figure 10.3 (left). However, in practice, as the errors are not very small, the histogram is skewed, as shown in Figure 10.3 (right).

A reason for why, under very small errors, the histogram tends to be approached by a normal distribution is the central limit theorem. This theorem states that, for a set of independent and random variables having a mean and a variance, the probability density function of the sum of the variables approaches a normal distribution as the number of variables increases. A reason for why the histogram becomes skewed when the errors become larger is that, as the lens has been optimized, most combinations of changes

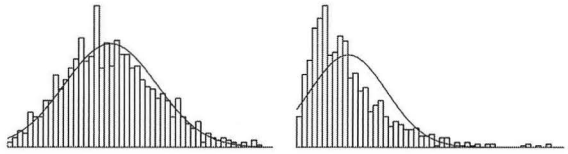

Figure 10.3 Left, histogram of RMS spot size for 1,000 Cooke triplets under very small fabrication errors. Right, histogram of the Cooke triplets under large fabrication errors. A best fit normal distribution has been overlaid with the histograms.

will tend to degrade the performance, and very few, or none, will tend to improve it.

For simplicity, a first estimate for the probability density function, $p(S)$, of a tolerancing criterion, S, is a normal distribution defined by,

$$p(S) = \frac{1}{\sigma_S \sqrt{2\pi}} \exp\left\{\frac{-(S - \langle S \rangle)^2}{2\sigma_S^2}\right\}, \tag{10.1}$$

where $\langle S \rangle$ is the mean, and σ_S^2 is the variance. The mean can be estimated by,

$$\langle S \rangle = S_0 + \sum_{i=1}^{j} \langle \Delta S_i \rangle, \tag{10.2}$$

where S_0 is the nominal value for the criterion, $\langle \Delta S_i \rangle$ is the mean of the change of the criterion S, due to the error in the parameter i out of a number of j parameters. For small errors, the mean would approach the nominal performance, $\langle S \rangle = S_0$. The variance can be estimated by,

$$\sigma_S^2 = \sum_{i=1}^{j} \sigma_i^2, \tag{10.3}$$

where σ_i^2 is the variance of the change of criterion S, due to the error in the parameter i.

10.7 RSS Rule

Out of the variance, σ_S^2 follows the Root Sum Square (RSS) rule. This estimates the standard deviation of the probability density function of the criterion. By using the square of the criterion change, ΔS_i^2, due to the parameter, i, instead of the variance, σ_i^2, the RSS rule is written as,

$$\sigma_S \cong \sqrt{\sum_{i=1}^{j} \Delta S_i^2}. \tag{10.4}$$

The RSS rule provides the following insights. First, the statistical worst case estimate for n errors that produce the same criterion changes is $\sqrt{n}\Delta S_i$; this is not as pessimistic as adding all the changes as $n\Delta S_i$. Second, it is the large criterion changes that count much more as they enter as their squares. Thus, if we have ten parameters that produce changes of 1, and one parameter that produces a change of 10, the RSS rule indicates that the impact on the standard deviation of the former parameters is $\sqrt{10}$, while the impact of the latter parameter is $\sqrt{100}$.

The RSS rule also helps to allocate tolerance budgets to different aspects of a lens system. For example, for a diffraction limited system, the total allowed wavefront error budget might be set to 0.0707λ RMS. This budget is allocated according to the RSS rule as 0.03λ RMS for the lens design, 0.04λ RMS for the assembly, and 0.05λ RMS for the fabrication ($0.03^2 + 0.04^2 + 0.05^2 = 0.0707^2$).

10.8 Monte Carlo Simulation

In a Monte Carlo simulation the constructional parameters of a lens are chosen randomly from ranges defined by the nominal parameter values and their error probability distribution. The parameters in error are used to construct a lens trial, compensators are applied, and the system tolerancing criterion change is determined. Many Monte Carlo trials are done to determine the statistics of the tolerancing criterion change. The mean of the tolerancing criterion and its standard deviation are determined from the list of criterion changes. Depending on the application a Monte Carlo simulation may start with 100 trials to check for the appropriateness of the lens modeling, then 1,000 trials, or more. As the trials increase, it is expected that the mean and the standard deviation converge as the square root of the number of trials, $\sqrt{\#trials}$. A rule of thumb is to execute a number of trials in the order of the square of the number of parameters under error. The modeling of a lens system for tolerancing can be an art and a science, as it can be quite elaborated to properly reflect the environment, materials, fabrication and assembly errors, and more. As the lens system must be optimized for each trial using the compensators as variables, Monte Carlo simulations may take long times to run. At the end, the goal is obtaining the statistics of the as-built lens and to assign tolerances for fabrication.

Table 10.4 *Monte Carlo trials, nominal criterion 0.34λ RMS, mean 0.421λ RMS, standard deviation 0.047λ RMS*

Trial #	Criterion	Change
1	0.441	0.101
2	0.480	0.140
3	0.369	0.029
4	0.396	0.056
5	0.445	0.104
6	0.409	0.069
7	0.390	0.050
8	0.357	0.017
9	0.516	0.175
10	0.403	0.063

Each parameter error may have its own probability density function, such as uniform, truncated normal, end-limited, and others. Once the lens trial is constructed with the parameters in error, the lens is optimized using the compensators. When lens decenters, or surface tilts, are lens errors, the lens loses its axial symmetry and, therefore, it is important to properly sample the field of view to determine correctly the tolerancing criterion such as RMS spot size, or RMS wavefront error.

10.9 Monte Carlo Simulation Example

Consider a Cooke triplet lens, as shown in Figure 10.2. The focal length is $f' =$ 50 mm, the field of view (FOV) is ±24 degrees, and the optical speed is *F*/5. The tolerances assigned are: thickness ±0.1 mm, radius ±2.5 fringes, index ±0.0005, surface figure ±0.5 fringe, and surface tilt ±1.5 arc-minutes. A truncated normal distribution for these errors is assumed. The field of view is sampled at the field center and four full field positions. The back focal length was used as a compensator. A lens decenter can be decomposed as two surface tilts and a thickness change. However, for small surface tilts the thickness change is negligible. Thus, for simplicity and clarity, here only surface tilts in two directions are allowed.

Table 10.4 shows the results of ten Monte Carlo runs, which give a mean value of 0.421λ RMS, and a standard deviation of 0.047λ RMS. The nominal wavefront error is 0.34λ RMS. Depending on the performance requirements, on the parameters that most degrade the tolerancing criterion, the optics shop's ability to meet tolerances, and cost, the tolerances can be made tighter or looser

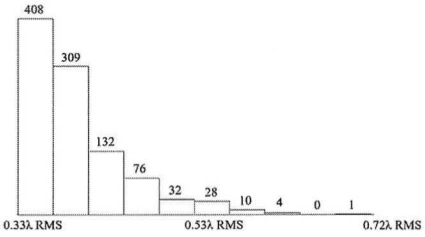

Figure 10.4 Histogram of 1,000 Monte Carlo runs for a Cooke triplet lens.

to meet the requirements and cost. This is a simple example to illustrate how the tolerancing criterion statistics are obtained. However, for a lens to be manufactured the tolerancing process is often elaborated to properly model the as-built lens.

Figure 10.4 shows the histogram of 1,000 Monte Carlo trials for the same Cooke triplet lens, the mean value is 0.4λ RMS, and the standard deviation is 0.055λ RMS. Each histogram bin has trials with performance within about 0.04λ RMS. Thus, there are 408 lens trials with a tolerancing criterion between 0.33λ RMS and 0.37λ RMS. Therefore, under the tolerances specified there is a percentage probability of about 40.8% that the lenses will perform within 11.8% from the nominal performance. Also, there is a probability of 71.7% that the lenses will perform within 23.6% from the nominal performance. If uniform distributions are chosen for the parameters then the mean would be 0.42λ RMS and the standard deviation would be 0.077λ RMS. Thus, properly modeling the parameters error distribution provides a more accurate level of tolerancing.

Because the errors in the fabrication of a lens can substantially degrade the lens performance, it is important to minimize as much as possible the nominal tolerancing criterion during the lens optimization, so that there is more room to accommodate for such errors. However, different forms of optical systems that satisfy the requirements for an application may have more or less sensitivity to fabrication errors for the same level of nominal image quality.

Table 10.5 provides the mean and standard deviation when 1,000 trials at a time were performed for a given category of error. The change in the mean of the tolerancing criterion for errors in thickness, as well as its standard deviation, are large. Clearly, and by far, the worst offender is the category of thickness errors. Tightening the tolerance in thickness will be a choice. For example, by decreasing the thickness tolerance to ±0.05 mm, the criterion mean would be 0.34λ RMS, and the standard deviation would be 0.016λ RMS. This would make 81% of the lenses perform within 10% of the nominal

Table 10.5 *Cooke triplet lens. Mean and standard deviation for categories of errors, nominal mean 0.328λ RMS*

Parameter category	Mean λ RMS	Standard deviation λ RMS
Radius	0.329	0.0038
Thickness	0.378	0.0520
Surface tilt	0.334	0.0056
Figure	0.328	0.0033
Index	0.328	0.0022

Table 10.6 *Constructional data of the Cooke triplet lens,* f = *50 mm, FOV* = ±*24°, F/5*

Surface	Radius (mm)	Thickness (mm)	Glass
1	26.6335	3.25	N-LAK33
2	426.1623	6.0	
3 (Stop)	−25.9915	1.0	TIF6
4	25.0718	4.75	
5	169.8704	3.0	N-LAK33
6	−23.2263	42.3551	

criterion. However, lens manufacturers put a cost premium on tight tolerances for thickness because of the risk of over-grinding the lens and the need to start over with a new blank lens. A next step would be to explore using the airspaces as compensators to avoid tightening the lens thickness tolerance. This might result in a tedious and costly lens assembly. Table 10.6 provides the constructional data of the Cooke triplet. Thus, increasing the lens production yield is most often a trade-off with cost.

10.10 Behavior of a Lens under Manufacturing Errors

Under fabrication errors, that is under lens perturbation, a lens system suffers from a number of optical effects. These can be divided as relating to axial symmetry and not relating to axial symmetry. Errors in radii of curvature, lens thickness, and index of refraction maintain the axial symmetry of a lens. Errors in surface tilt break the axial symmetry.

The first-order effects to take place are that the focal length changes, and that the image is displaced laterally. This lateral image displacement is known as bore-sight error, or line of sight error, and arises from the lenses becoming

Table 10.7 *Changes that take place under perturbation according to symmetry and to aberration order*

Changes that relate to axial symmetry		Changes that relate to lack of axial symmetry	
First-order	Aberration	First-order	Aberration
Focal length	Spherical aberration	Image lateral displacement	Uniform coma
Image size	Linear coma aberration	Anamorphic image distortion	Uniform astigmatism
		Chromatic change of line of sight	Linear astigmatism
			Field tilt

wedged. In addition, for each wavelength, the image displacement might be different. The second effects that take place are changes in the aberrations, and that new aberrations appear. Table 10.7 provides a summary of these effects according to the symmetry, and whether they are of first-order, or relate to aberrations. In the same way that spherical aberration W_{040} is uniform over the field of view, uniform coma and uniform astigmatism can now be present over the field of view. Linear coma W_{131} grows linearly with the field of view; now linear astigmatism and linear focus, this is field tilt, can take place.

The change in focal length of a thin lens is given by,

$$\Delta \mathrm{f} = \frac{\Delta \mathrm{n}}{n-1} f. \tag{10.5}$$

A change in the index of refraction of 0.001 results in a change of focal length of approximately 0.2%. Index of refraction can be measured to 1×10^{-5}, and is usually sufficiently well known. Thus, system changes due to errors in the index of refraction are expected to be very small. However, for diffraction limited systems it is important to check the index of refraction of the materials being used. The index of refraction homogeneity is also of concern, as a difference in index of 0.0001 in a 10 mm glass blank produces an optical path difference of 0.001 mm, or about two wavelengths in the visible spectrum.

Having an understanding of the effects that take place when a lens is perturbed can allow a lens designer to control, or mitigate, them to avoid specifying tight tolerances. For example, the tilt of an image sensor can be used to match field tilt aberration, or some radial adjusting screws can be designed into a lens barrel to laterally displace a lens and correct for uniform

Table 10.8 *Lens configuration setting for desensitizing a Cooke triplet lens for lens element and tilt errors*

Configuration	1	2	3	4	5	6	7
Focal length, mm	100						
Lens #1 decenter, mm		0.025					
Lens #2 decenter, mm			0.025				
Lens #3 decenter, mm				0.025			
Lens #1 tilt					0.05°		
Lens #2 tilt						0.05°	
Lens #3 tilt							0.05°

coma. This has been done in adjusting microscope objectives. Alternatively, a lens airspace can be adjusted to correct for residual spherical aberration.

Uniform astigmatism depends on the square of the surface tilt. Since the lens tilts under consideration are small, uniform astigmatism is negligible. Thus, if this aberration is detected in a nominally axially symmetric lens system, it is likely due to surface figure error or to a lens being deformed due to improper mounting. Table 1 in Appendix 4 summarizes the primary aberrations that can take place in a plane symmetric system.

10.11 Desensitizing a Lens from Element Decenter, Tilt, or Wedge

Lens design programs allow us to set multi-configurations for a lens system. Each configuration may differ, for example, in constructional parameters, in field of view, in relative aperture, and in wavelength choice. An opto-mechanical engineer is concerned about lens decenter and tilt tolerances. To desensitize a lens, say a Cooke triplet lens, seven configurations are defined. One configuration is the nominal configuration; three configurations are for lens element decenter, one for each lens; and three configurations are for lens element tilt, one for each lens; this setting is shown in Table 10.8. The error function for the nominal configuration has the first-order lens constraints and may include image quality performance. The error function for the remaining six configurations has only image quality performance.

Lens decenters and lens tilts are set only in one direction, so as to reduce the lens system symmetry to plane symmetry. The field of view needs to be properly sampled, as there is no longer axial symmetry for six configurations. However, because the system becomes plane symmetric and the main effects

Table 10.9 *Lens configuration setting for desensitizing a Cooke triplet lens for lens wedge*

Configuration	1	2	3	4	5	6	7
Focal length, mm	100						
Surface #1 tilt		0.1°					
Surface #2 tilt			0.1°				
Surface #3 tilt				0.1°			
Surface #4 tilt					0.1°		
Surface #5 tilt						0.1°	
Surface #6 tilt							0.1°

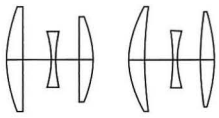

Figure 10.5 Desensitized Cooke triplet lens. Left, standard lens solution; Right, desensitized lens solution. The front positive lens takes a meniscus form, and the rear positive lens takes a double convex form. Glasses are N-LAK33, TIF6, and N-LAK33. FOV = ±24° at *F*/5.

of surface tilt are uniform coma and linear astigmatism, sampling three or five fields in the plane of symmetry might be sufficient. Then optimizing such a multi configuration lens system will tend to desensitize the lens system for lens element decenter and tilt errors. Performance gains of 5%, 10%, or more are often obtained. If the desensitizing is not sufficient, then a different lens solution is desensitized and evaluated until the specified lens yield is achieved for a given set of tolerances. In this desensitizing method, the lens optimizer will change the lens to mitigate the worst offenders to performance first, due to lens element decenter and tilt errors. Compensators can be added by releasing as variables appropriate lens parameters, such as the back focal length, the image plane tilt, or a lens decenter.

For spherical surfaces a lens decenter can be resolved as two surface tilts and a thickness change; however, the thickness change is negligible.

The optics shop is concerned about lens wedge tolerances. Lens system desensitizing for a lens wedge can be done by tilting each of the surfaces of a lens system in a multi-configuration, as shown in Table 10.9 for a Cooke triplet lens. Then optimization under surface tilt perturbation may provide a desensitized lens. Figure 10.5 shows the form of a Cooke triplet lens that has been desensitized to surface tilt. The main offender to the performance of the Cooke triplet was sensitivity to linear astigmatism, which was mitigated. In this case it

was necessary to set each surface tilt first to 1.0° and then to 0.1° for the optimizer to escape from a standard solution and find the less sensitive lens solution.

10.12 Lens Drawings

Once a lens is designed and tolerances have been assigned for manufacturing, lens drawings need to be produced. A lens drawing should provide sufficient information so that the correct lens is made. It is important to have effective communication with the lens manufacturer to reflect the shop fabrication skills and to avoid mistakes.

Further, it is imperative that the lens designer checks, and double checks, a lens design to make sure there are no errors. A lens designer needs to also have effective communication with the opto-mechanical engineer who will design the lens barrel, and the lens assembly engineer, to make sure the lens can be made and be assembled and aligned.

There are a variety of lens formats for lens drawings according to organization or company. However, a sample of the International Organization for Standardization (ISO) standard for drawings for optical elements and systems, ISO 10110-10, is shown in Figure 10.6.

In addition to the lens drawing in the top of Figure 10.6, the three boxes in the bottom are for providing the following information, for each surface and for the material: Material type, index of refraction, and ν-number; Radius of curvature, convex CX, concave CC, and tolerance; Clear aperture or optically effective diameter; Protective chamfer; Surface treatments and coatings; Stress

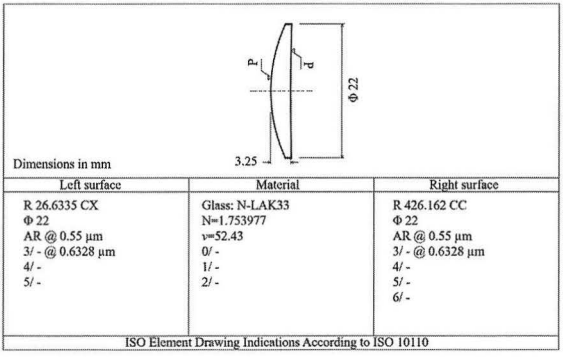

Figure 10.6 Lens drawing according to ISO 10110-10.

birefringence; Permissible bubbles and other glass inclusions; Glass homogeneity; Surface irregularity; Centering tolerance, or wedge; Surface imperfections allowance; Laser damage threshold indication; and Whether the surface is cemented or optically contacted.

Further Reading

Bates, R. "Performance and tolerance sensitivity optimization of highly aspheric miniature camera lenses," *Proceedings of SPIE*, 7793 (2010), doi: 10.1117/12.860919.

Bauman, Brian J., Schneider, Michael D. "Design of optical systems that maximize as-built performance using tolerance/compensator-informed optimization," *Optics Express*, 26 (2018), 13819–40.

Fuse, K. Method for designing a refractive or reflective optical system and method for designing a diffraction optical element, USP 6,567,226 (2003).

Grey, D. S. "Tolerance sensitivity and optimization," *Applied Optics*, 9(3) (1970), 523–26.

Herman, E., Sasián, J. "Aberration considerations in lens tolerancing," *Applied Optics*, 53 (2014), 341–46.

Rimmer, M. "Analysis of perturbed lens systems," *Applied Optics*, 9(3), (1970), 533–37.

Rogers, J. "Using global synthesis to find tolerance-insensitive design forms," Proceedings of SPIE 6342, International Optical Design Conference 2006, 63420M (2006), doi: 10.1117/12.692251.

Rogers, J. "Global optimization and desensitization," Proceedings of SPIE 9633, Optifab 2015, 96330S (2015), doi: 10.1117/12.2196010.

Sasián, J., McCormick, F. B., Webb, R., Crisci, R. J., Mersereau, K. O., Stawicki, R. P. "Design, assembly, and testing of an objective lens for a free-space photonic switching system," *Optical Engineering*, 32(8) (1993), 1871–78.

Schwiegerling, J. *Optical: Specification, Fabrication, and Testing* (Bellingham, WA: SPIE Press, 2014).

Smith, W. J. "Fundamentals of establishing an optical tolerance budget," *Proceedings of SPIE, Geometrical Optics*, 0531 (1905), 196–204.

Weichuan, Gao, Youngworth, Richard N., Sasián, José. "Method to evaluate surface figure error budget for optical systems," *Optical Engineering*, 57(10) (2018), 105108.

Youngworth, R. N. "Statistical truths of tolerance assignment in optical design," *Proceedings of SPIE*, 8131 (2011), 81310E.

17
Miniature Lenses

There are a number of technological applications that use miniature lenses in which the lens diameter is a few millimeters, and typically smaller than 10 mm. For lens systems that employ such miniature lenses, several advantages result because of the scale. For a given lens form and, except for distortion, the aberrations scale down, while the wavelength of light remains the same. Given that lens volume is small, a wider possibility of lens materials becomes possible due to cost or material limitations. Lens weight is reduced, as well as dimensional changes due to temperature. Further, very thick lenses can be used in some applications. However, lens tolerances for lens thickness and decenter become tighter. Many microscope objectives, lenses for endoscopes, and lenses for mobile phones are in the category of miniature lenses. This chapter provides a discussion about lens design for mobile phones lenses.

17.1 Lens Specifications

Lenses for mobile phones, as illustrated in Figure 17.1, have been developed over the last two decades. Lens designs have evolved from having one or two lens elements, to three and four elements, to five-to-eight lens elements. Some of the lens elements have been made by glass molding, but currently they are made by plastic injection molding. To aid in the correction of aberration, highly aspheric surfaces are used. Table 17.1 provides typical lens specifications for field of view (FOV), focal length, F-number, total track length (TTL) from the vertex of the first surface of the lens to the image plane, chief ray angle of incidence at image sensor (CRA), relative illumination (RI), and number of lens elements.

Like any other photographic lens, the design of a mobile phone lens is driven by the light sensor; for example, a Charge Coupled Device (CCD) or

Table 17.1 *Typical mobile phone lens specifications*

Year	2006	2012	2018
Focal length	3–6 mm	3–5 mm	3–5 mm
FOV	66°	72°	78°
F/#	2.8	2.2–2.4	2.0–1.4
TTL	<5.0 mm	<5.0 mm	<6.0 mm
Distortion	<1–2%	<1–2%	<1–2%
CRA	<24°	<30°	<33°
RI	>50%	>50%	>32%
# lens elements	3–5	4–6	5–8

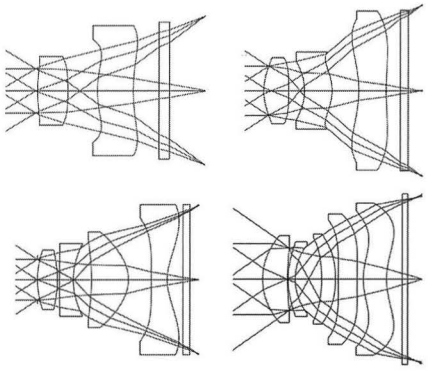

Figure 17.1 Mobile phone lens forms with two, three, four, and five lens elements. The plane parallel plate next to the image plane represents an infrared filter.

Complementary Metal Oxide Semiconductor (CMOS) image sensor. The diagonal of the active area of the sensor defines the minimum image circle diameter; some allowance in this diameter is given to allow for some lens/sensor decenter. There are many format sizes for an image sensor that are given in inches, such as 1/3″. This format has a diagonal of 6 mm, a width of 4.8 mm, and a height of 3.6 mm. The inch designation of image sensors is an arcane reference to the vidicon tubes used in early video cameras. It is best to look up the actual digital image sensor dimensions for a given sensor specification.

The lens design is also driven by the specified total track length, which is often required to be less than 6 mm, so that the lens can be integrated in a thin mobile phone. Although most designs for mobile phone lenses are not telephotos, the ratio of the total track lens to the focal length, the telephoto ratio, is still used. A typical value for this ratio is 1.2.

Table 17.2 *Example of MTF specifications in fractions of the Nyquist frequency and in cycles/mm for an object at infinity*

	N_Q	$N_Q/2$	$N_Q/4$
MTF On-axis	>40%	>60%	>80%
MTF Off-axis @ 0.7 field	S>30% T>20%	S>50% T>40%	S>70% T>60%
MTF Off-axis @ 1.0 field	S>20% T>10%	S>30% T>20%	S>40% T>30%

Given the focal length and the image circle diameter, and assuming no distortion, the field of view can be calculated. Thus, for a focal length of 4.8 mm and an image circle diameter of 6 mm, the field of view is ±32°.

Electronic sensors have pixels sensitive to the light incident on them. Typical pixel sizes for CMOS sensors vary in the range of 0.001 mm to 0.008 mm. A given spatial frequency can be recovered whenever it is sampled with twice that frequency. This sampling frequency is known as the Nyquist frequency, N_Q. An image sensor can sample an image at a spatial frequency of 1/(pixel size). It follows that the sensor can recover a spatial frequency, N_Q = 1/(2 × pixel size). If the pixel size is 1.5 μm, then N_Q = 333 cycles/mm (also line pairs per mm; lp/mm). The maximum frequency that a lens with a circular aperture can image is $N_C = 1/(\lambda F/\#)$. Using λ = 0.5 μm and F/2.2 yields N_C = 909 cycles/mm. Thus, a diffraction limited lens at F/2.2 would not limit the sensor spatial frequency sampling. The image quality for a lens can then be specified in terms of the Nyquist frequency, for different fields and object distances, as shown in Table 17.2.

The design of a mobile phone lens also requires consideration of the spectral bandwidth to be used, for example, the visible spectrum from 400 nm to 700 nm. A filter is used in mobile phone lenses to suppress infrared radiation (IR). This filter is modeled as a parallel plate of BK7 glass as the last element of the lens system. The filter introduces spherical aberration that must be compensated by a lens element near the stop aperture. In addition, the spectral response of the sensor is used to weight the wavelengths used by the lens optimizer to reflect the sensor's sensitivity to wavelength.

A CMOS sensor includes an array of micro-lenses, also called lenslets, placed on top of the light sensitive pixels. As shown in Figure 17.2, the function of each micro-lens is that of a field lens that forms an image of the exit pupil of the mobile phone lens onto the surface of each light sensitive element of a pixel. In this way, light is redirected to the active areas in each pixel, as not all the area of a pixel is light sensitive. The array of micro-lenses

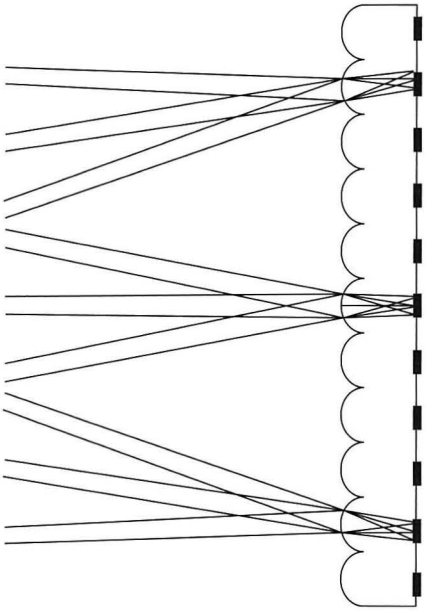

Figure 17.2 Model of array of micro-lenses to improve light coupling efficiency. The micro-lenses act as field lenses, forming a pupil at the CMOS light sensitive elements.

requires a specific chief ray angle (CRA) of incidence as a function of the ray height on the sensor. The specification can be simply to match a given CRA at the corner of the sensor, or to match within one or two degrees a table of angles of incidence as a function of the radial position on the sensor.

There must be enough back focal length (BFL) to allow placement of the image sensor and any clearances required by opto-mechanical considerations.

17.2 Lens Design Considerations

Mobile phone lenses have been evolutionary, in that every generation increased complexity from the previous one. The first-order layout in practice is usually taken from an existing lens design form. Given that lens element axial thickness can be substantial, thick lenses can be used, and more design forms are possible whenever the lens system has two or three lens elements, or when the total track length is not a concern. Many combinations of optical power for the lens elements are possible, for example PNPN, PNNP, NPPN for a four-lens element system. The patent literature has hundreds of lens

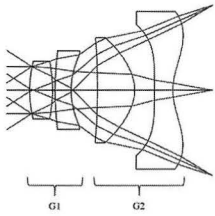

Figure 17.3 Four-lens element mobile phone lens. The first and second lens elements form the front group, and the third and fourth lens elements form the rear group.

design examples for mobile phone lenses and their forerunners, personal digital assistants.

Figure 17.3 shows a four-element mobile phone lens divided into two groups, G_1 and G_2. The stop aperture is placed in front to reduce the chief ray angle of incidence at the image sensor, or slightly inside the lens to help provide some lens symmetry and to reduce odd aberrations. However, provided the relative illumination specification is met, the stop aperture can be placed in front, and some vignetting by an aperture inside the lens can be allowed. This vignetting has the effect of making the stop aperture appear inside the lens for off-axis field points. For stray light control, several apertures are usually specified within the mobile phone lens assembly.

Significant optical power of the lens system is in the front lens group, which must provide the majority of the correction for chromatic aberration, spherical aberration, and coma. The rear group corrects for Petzval field curvature, astigmatism, and distortion aberration. This group usually has highly aspheric surfaces. In particular, the last aspheric surface changes the optical power, from negative near the optical axis to positive near the edge of the lens. This positive power helps to decrease the CRA and introduces positive pupil coma, which helps to increase the relative illumination. Pupil spherical aberration is also present due to the positive power of the last lens near the edge.

The total track of the lens system has a strong impact on imaging quality. The smaller the telephoto ratio is, the more difficult it becomes to meet image quality requirements, in part because the lens is optically stressed and higher order aberrations become larger.

It is good practice not to specify unnecessary aspheric terms and to keep them at a minimum number. If many aspheric terms are used, the lens optimizer may create surface features in one lens that are canceled in another lens. Under lens decenter, the features can partially add rather than cancel, with the result that the as-built-lens becomes more sensitive to manufacturing

errors. Lens elements near the stop aperture may need only two or three aspheric terms, as their function is mainly to correct for spherical aberration.

As mentioned before, one problem with the small scale of miniature lenses is that lens element thickness and decenter errors can have a large impact by decreasing performance. For example, a thickness error of 0.1 mm can be tolerable in a 50 mm focal length lens, but not at all in a miniature lens with a focal length of 5 mm. Therefore, an important part of the lens design is to desensitize as much as possible a given design. The wavefront and distortion correction should not have rapid changes at the edge of the aperture or field, or slightly beyond the image circle, that could substantially decrease the performance of the as-built lens. Minimizing ray angle of incidence over all the lens surfaces helps to make the lens system less sensitive to errors.

The first and second lens elements in the front group usually have strong optical power to correct for chromatic aberration and provide most of the system's optical power. Any manufacturing or assembling errors in these lens elements can introduce significant aberration that would degrade the image sharpness. Field correcting elements in the rear group have a small beam footprint and a large chief ray height, and, under manufacturing errors, they can introduce asymmetrical image distortion.

During the early stages of the design of a mobile phone lens, and to explore possible lens forms, the surface conic constant and the fourth order aspheric coefficients can be released as variables for optimization. Once a promising design form is found, more aspheric terms can be added, provided they contribute to improve performance. It is important that, for optimization and evaluation, sufficient pupil and field sampling points be specified. Typically, the field is sampled with at least ten field points.

The optimization of a mobile phone lens can start with minimizing RMS spot size, then minimizing RMS wavefront error, and finally adjusting the lens to meet MTF requirements. If a given design form cannot meet image quality specifications, then a lens designer may consider changing lens materials or adding one more lens element. To add a lens element, a parallel plate of zero thickness is inserted in an air space, or a thick lens is split into two lenses with no air space between them. Fourth-order aspheric terms are included in the new surfaces, and the system is re-optimized, not necessarily allowing the radii of the new surfaces to vary. Then thickness is added to the new surfaces by small increments until a lens that is physically possible, this is with positive thicknesses and non-overlapping lenses, is obtained. As lens complexity is added, more design forms are possible, and lens image quality is expected to improve. The lens form of Figure 17.3 has been used as a starting point in many patented lenses to develop designs with more lenses. Parallel plates of

Table 17.3 *Example of a four-lens element design for a mobile phone lens. f′ = 5.0 mm, FOV = ±32°, TTL/f = 1.4,* F/2.8, *CRA = 30.6°*

Surface	Radius	Thickness	Plastic	K	A_4
STOP					
2	3.5432.72	0.87	E48R	−3.2457	
3	−4.57977	0.1		−11.7213	
4	126.2449	0.6	OKP4	0.0	
5	3.013807	0.8		−0.9977	-2.533×10^{-3}
6	−8.81693	1.61	E48R	0.0	4.161×10^{-3}
7	−1.61409	1.0		−2.2699	−0.0126713
8	72.73421	0.7	OKP4	0.0	−0.0100888
9	2.101288	0.7		−6.3020	-6.073×10^{-3}
10	Plano	0.3	BK7		
11	Plano	0.4			
Image					

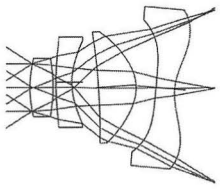

Figure 17.4 Example of a lens system with exaggerated lens element decenter and tilt.

glass have been added and then optimized to obtain five, six, and seven element designs.

Lens desensitizing to manufacturing errors is still an important requirement, so that the as-built lens meets fabrication yield specifications. Figure 17.4 shows exaggerated lens decenter and tilt, which can happen during lens assembly. Under lens element decenter and tilt, the axial symmetry is broken, and new aberration forms can appear. For example, in addition to uniform spherical aberration, uniform coma and uniform astigmatism can take place. In addition to linear coma, linear astigmatism and field tilt can also take place. Further, in addition to cubic distortion, asymmetric quadratic distortion can take place. Here uniform refers to the aberration being independent of the field of view, linear as dependent linearly with the field, and so forth. Appendix 4 provides a table of aberrations that can happen when the lens symmetry is reduced from axial to plane symmetry.

An example of a four-lens element design is given in Table 17.3 and shown in Figure 17.1 (bottom left). In this design, only conic constants and

fourth-order coefficients of asphericity were used. This is to emphasize that the use of many higher order aspheric coefficients, such as up to sixteenth order, may not be necessary as they can be redundant.

It is common to have errors in the aspheric coefficients due to truncating numbers, incorrect algebraic signs, neglecting numbers, or swapping coefficients. Thus, typically a lens, say from the patent literature, would need to be re-optimized to correct errors, to reflect actual indices of refraction, to adjust focal length, field of view, optical speed, MTF performance, and to reflect current manufacturing requirements such as minimum central and edge thicknesses.

17.3 Lens Manufacturing Considerations

Early lens systems used glass for the first lens element to provide a large ν-number difference for the correction of chromatic aberration, and for making the lens system less sensitive to environmental changes such as temperature and humidity variations. However, with the development of plastic materials with low ν-numbers, low birefringence, low water absorption, and the introduction of auto-focus, lens systems with all the lens elements made by plastic injection molding have been realized.

Under large volume production, lenses made by plastic injection are preferred to lenses made by glass molding, because of cost. Some advantages of plastic lens molding are the freedom to specify aspheric surfaces, and the choice to specify a lens flange to help precisely position a lens element with respect to other lens elements, thereby simplifying the lens system assembly.

For proper plastic flow and cooling, plastic lens manufacturers have some requirements for the aspect ratio of positive and negative lenses. Some guidelines are as follows: for positive lenses the ratio of lens central thickness to edge thickness should not be more than 3.2, and the edge thickness should not be less than 0.32 mm; for negative lenses the ratio of the maximum thickness to the central thickness should not be larger than 2.7, and the central thickness should not be less than 0.27 mm. These requirements are over the clear aperture of the lens and do not consider the lens flange; they are intended for the lens designer. Further, they also depend on the capabilities of the manufacturer. The ideal lens for injection molding approaches a lens with parallel surfaces so that plastic flow, cooling, and shrinkage are uniform. For miniature lenses, tolerances of 10 μm for thickness, decenter, total indicator runoff, and lens tilt are low; tolerances between 2 μm and 5 μm are medium and feasible to achieve in manufacturing, and tolerances between 0.5 μm and 2 μm are challenging to achieve, and are met for some miniature optics.

Table 17.4 *Properties of some plastics used in mobile phone lenses*

Code	n_d	v	γ	ρ
480R	1.525	55.95	$+1.44 \times 10^{-4}$	1.01
E48R	1.531	56.04	-2.62×10^{-4}	1.02
F52R	1.534	57.09	-2.21×10^{-4}	1.01
OKP4	1.607	26.90	-3.44×10^{-4}	1.20
OKP4HT	1.632	23.33	-2.72×10^{-4}	1.24

n_d, index of refraction; v, v-number; γ, opto-thermal coefficient; ρ, specific gravity.

The optical and mechanical properties of some plastics used in miniature lens systems are shown in Table 17.4. Some advantages of plastics over glass are that they are moldable at a lower temperature, have lower cost for large volumes, with lower weight, and aspheric and diffractive surfaces can be specified. Some disadvantages are the greater sensitivity to temperature changes, increased sensitivity to water absorption, internal light scattering or haze, reduced light transmission below 450 nm and above 1,000 nm, and a low resistance to abrasion.

Further Reading

Bareau, Jane, Clark, Peter P. "The optics of miniature digital camera modules," Proceedings of SPIE 6342, International Optical Design Conference 2006, 63421F (2006), doi: 10.1117/12.692291.

Clark, P. "Lens design and advanced function for mobile cameras," Chapter 1, in *Smart Mini-Cameras*, Galstian, T. V., ed. (Boca Raton, FL: CRC Press, 2014).

Clark, Peter P. "Mobile platform optical design," Proceedings of SPIE 9293, International Optical Design Conference 2014, 92931M (2014), doi: 10.1117/12.2076395.

Reshidko, D., Sasián, J. "Optical analysis of miniature lenses with curved imaging surfaces," *Applied Optics*, 54(28) (2015), E216–23.

Schaub, M. *The Design of Plastic Optical Systems* (Bellingham, WA: SPIE Press, Vol. TT80, 2009).

Sure, Thomas, Danner, Lambert, Euteneuer, Peter, Hoppen, Gerhard, Pausch, Armin, Vollrath, Wolfgang. "Ultra-high-performance microscope objectives: the state of the art in design, manufacturing, and testing," Proceedings of SPIE 6342, International Optical Design Conference 2006, 63420E (2006), doi: 10.1117/12.692202.

Yan, Yufeng, Sasián, José. "Miniature camera lens design with a freeform surface," Proceedings of SPIE 10590, International Optical Design Conference 2017, 1059012 (2017), doi: 10.1117/12.2292653.

Links to optical plastics vendors:
http://www.ogc.co.jp/e/products/fluorene/okp.html
https://www.zeonex.com/Optics.aspx.html#glass-like

Index

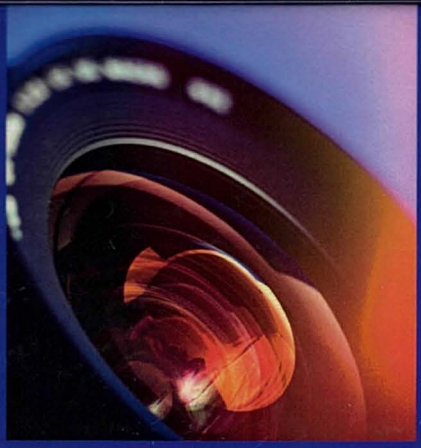

Optical lenses have many important applications, from telescopes and spectacles, to microscopes and lasers. This concise, introductory book provides an overview of the subtle art of lens design. It covers the fundamental optical theory, and the practical methods and tools employed in lens design, in a succinct and accessible manner. Topics covered include first-order optics, optical aberrations, achromatic doublets, optical relays, lens tolerances, designing with off-the-shelf lenses, miniature lenses, and zoom lenses. Covering all the key concepts of lens design, and providing suggestions for further reading at the end of each chapter, this book is an essential resource for graduate students working in optics and photonics, as well as for engineers and technicians working in the optics and imaging industries.

JOSÉ SASIÁN is Professor of Optical Design at the James C. Wyant College of Optical Sciences at the University of Arizona in Tucson, AZ. He has taught a course on lens design for more than 20 years and has published extensively in the field. He has worked as a consultant in lens design for the optics industry, and has been responsible for the design of a variety of successful and novel lens systems.

Cover image: courtesy of Getty Images.
iStock/dem10

COVER DESIGNED BY HART McLEOD LTD

CAMBRIDGE
UNIVERSITY PRESS
www.cambridge.org

ISBN 978-1-108-49432-8

9 781108 494328

CUP/V OPTICS/PHOTONICS
IPR2020-00905
027
74